SAND2016-4087PE

Exceptional service in the national interest

Sandia National Laboratories

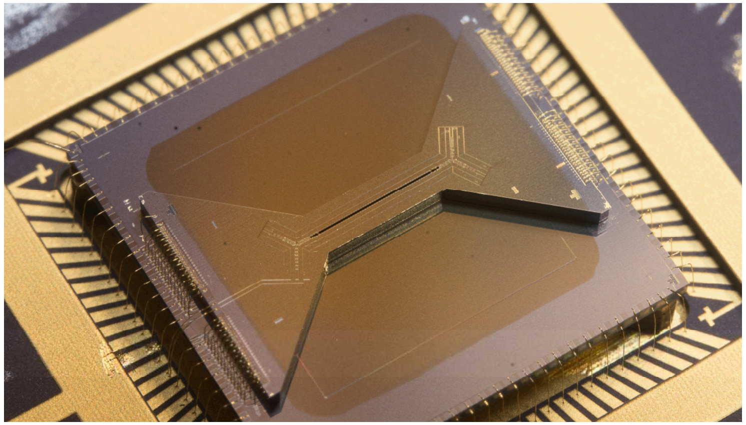

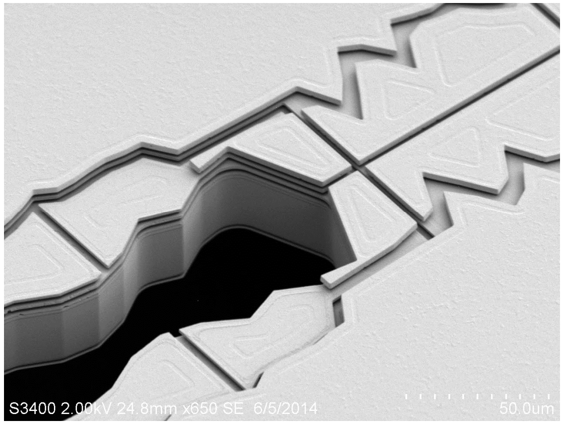

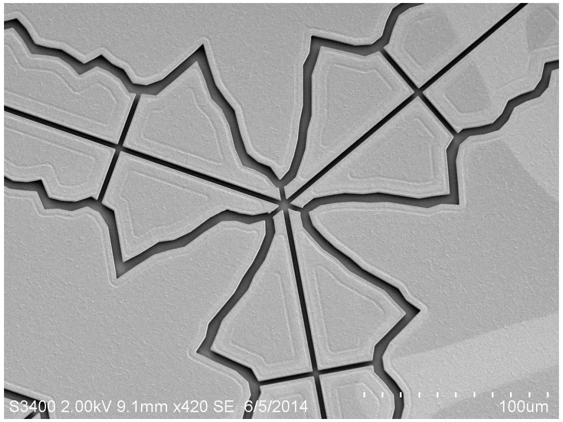

High-Fidelity Two-Qubit Quantum Gates in a Scalable Surface Ion Trap

Peter Maunz
Sandia National Laboratories

IARPA

LDRD LABORATORY DIRECTED RESEARCH & DEVELOPMENT

U.S. DEPARTMENT OF ENERGY

NNSA National Nuclear Security Administration

Sandia National Laboratories is a multi-program laboratory managed and operated by Sandia Corporation, a wholly owned subsidiary of Lockheed Martin Corporation, for the U.S. Department of Energy's National Nuclear Security Administration under contract DE-AC04-94AL85000.

Sandia National Laboratories

Micro-fabrication

- Microfabrication enables scalable traps
  - Junctions and transitions

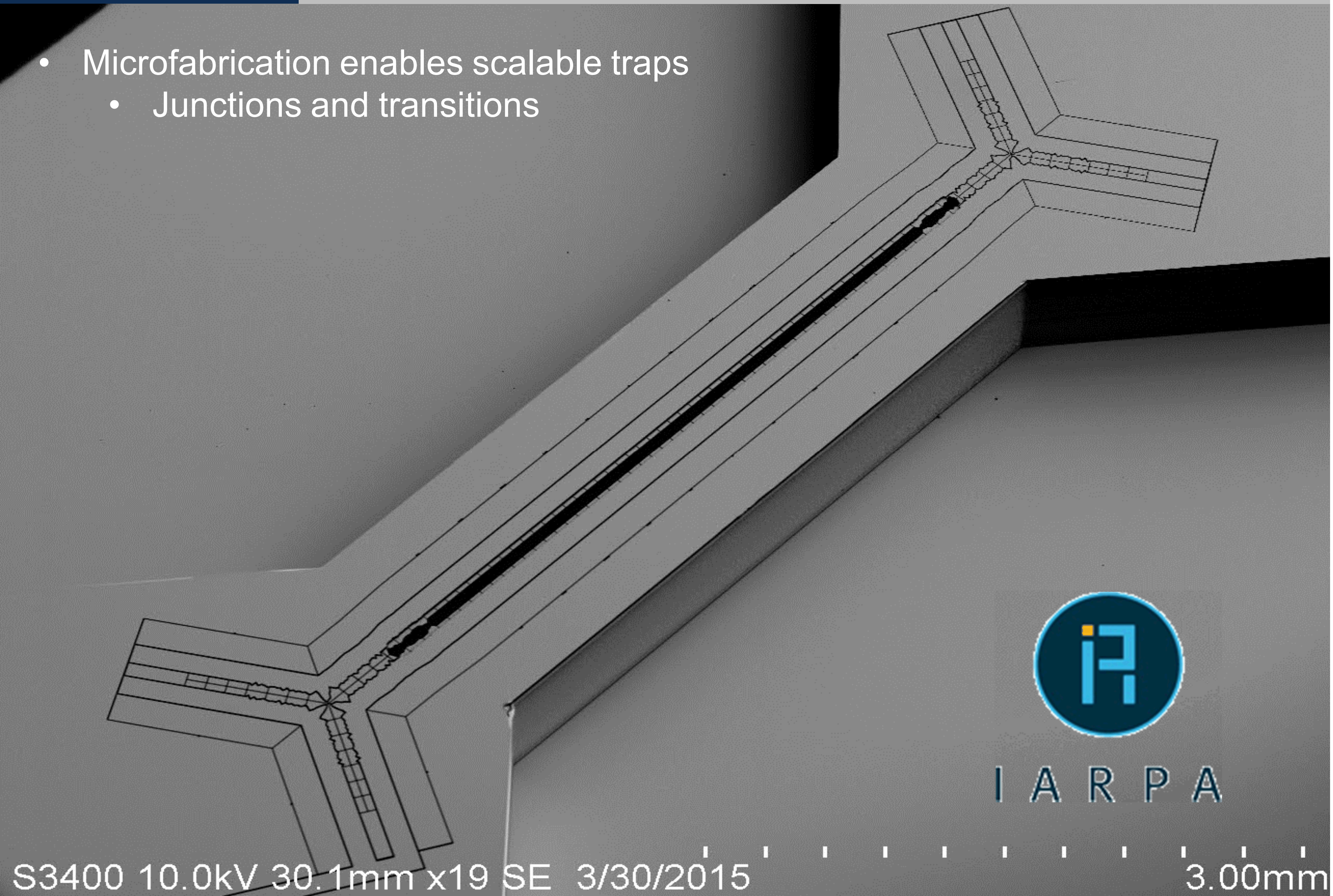

Challenges of surface traps

- Microfabrication enables scalable traps
  - Junctions and transitions
- Small distance to electrodes
  - Higher anomalous heating
- Nearby dielectrics
  - Possibly charging of the trap due to scattered laser light
- Small features
  - Sensitive to dust
- Higher anharmonic contributions to trap potential

Optimize traps for quantum information processing

We will demonstrate that microfabricated surface traps can be used for high fidelity quantum operations

IARPA

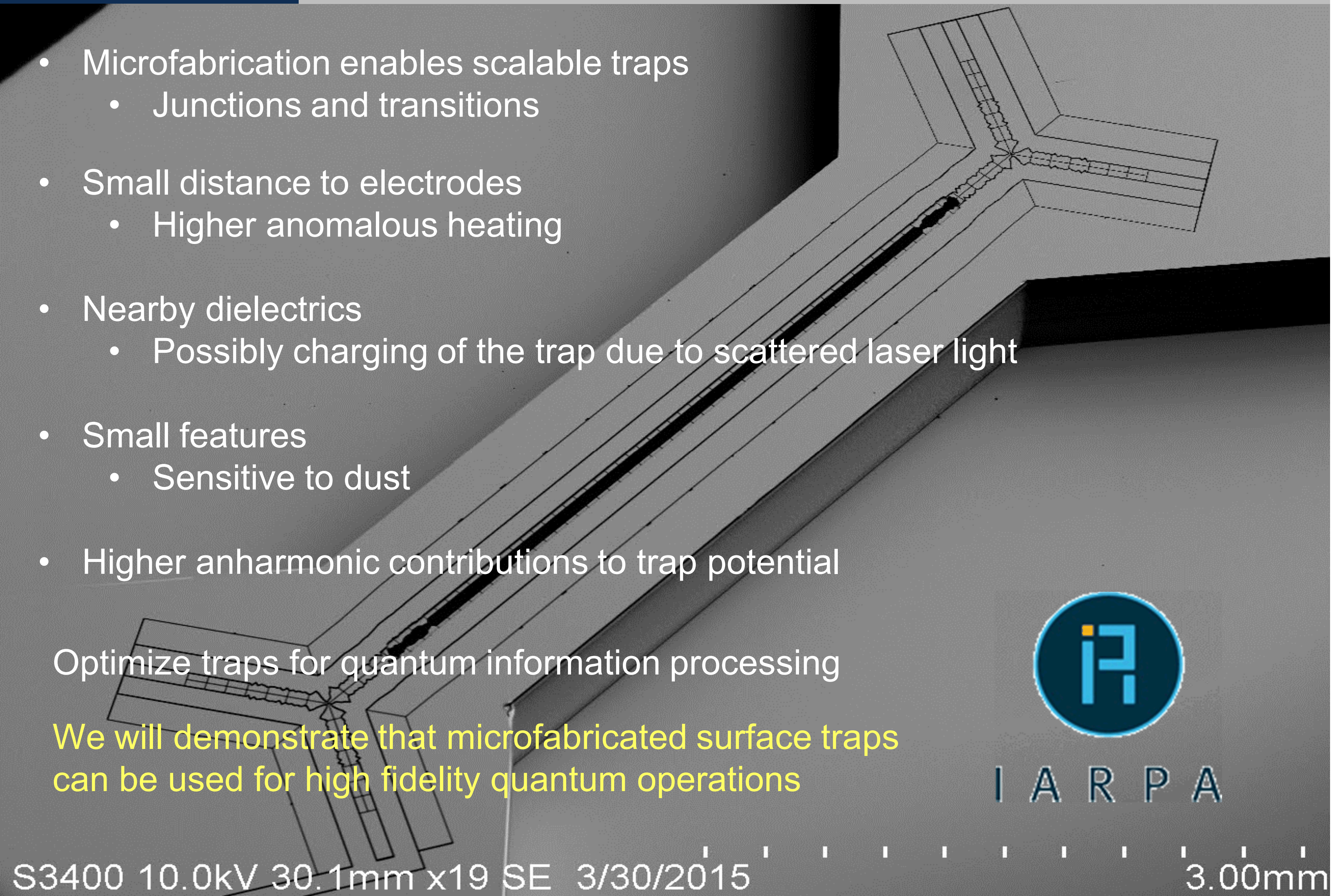

Outline

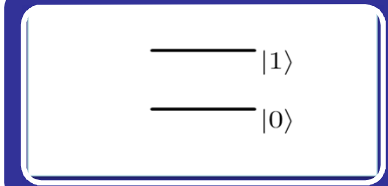

The ytterbium qubit

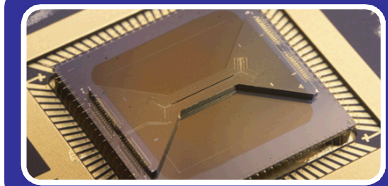

Sandia's HOA-2 trap

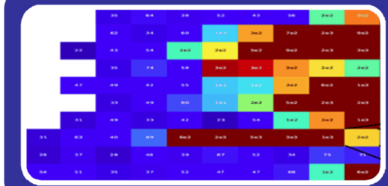

Characterization of quantum gates using GST (Robin Blume-Kohout)

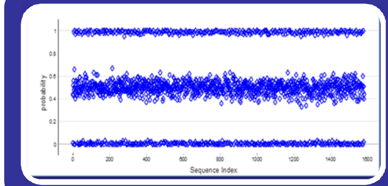

Single qubit gates

- Microwaves
- Raman transitions

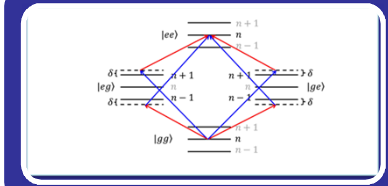

Characterization of the Mølmer-Sørensen two-qubit gate

The Ytterbium Qubit

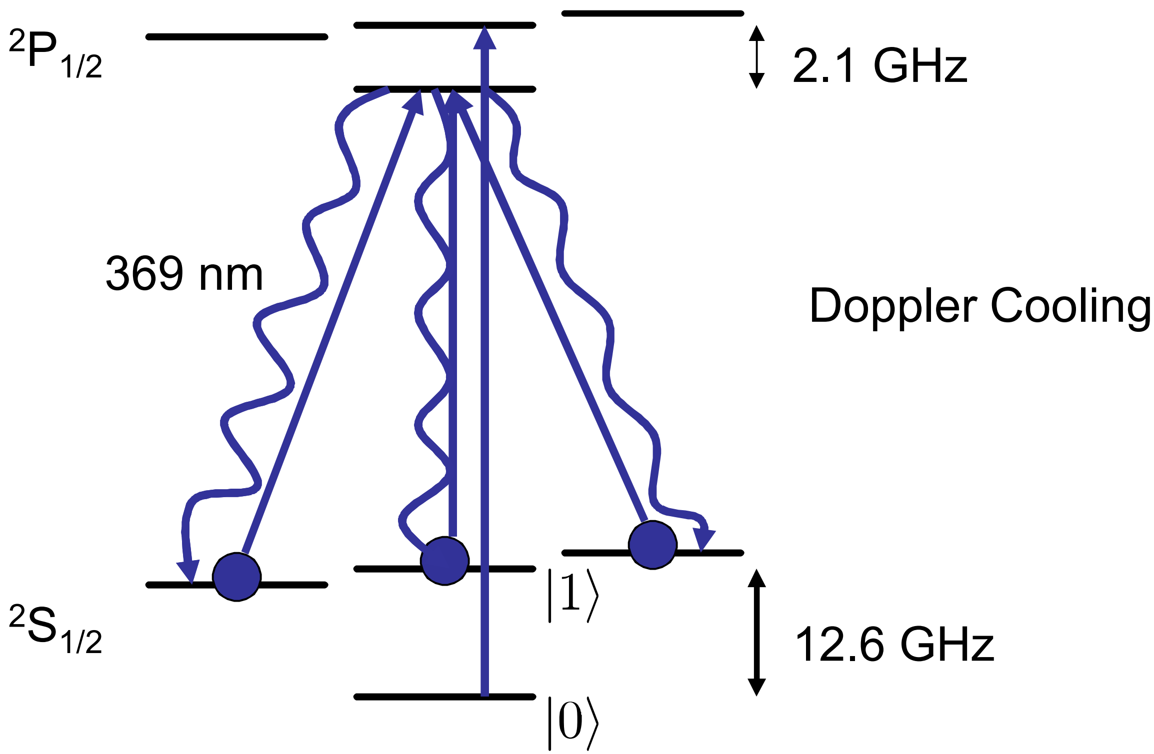

clock state qubit, magnetic field insensitive.

S. Olmschenk *et al.*, PRA **76**, 052314 (2007)

state initialization

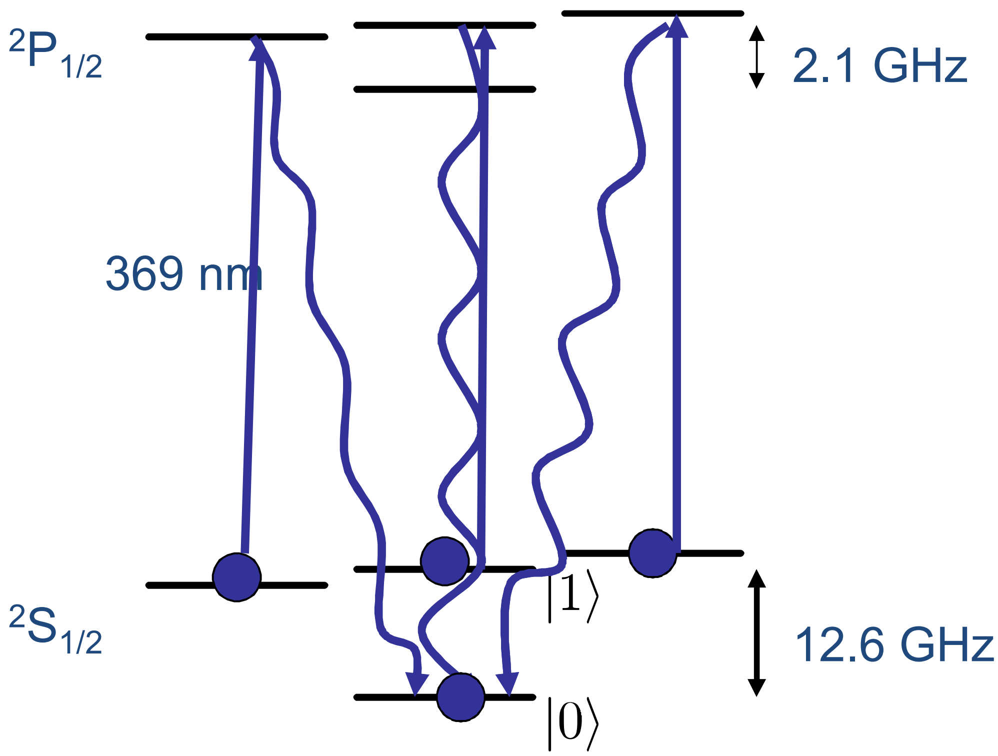

clock state qubit, magnetic field insensitive.

S. Olmschenk *et al.*, PRA **76**, 052314 (2007)

$^{171}Yb^{+}$ state detection

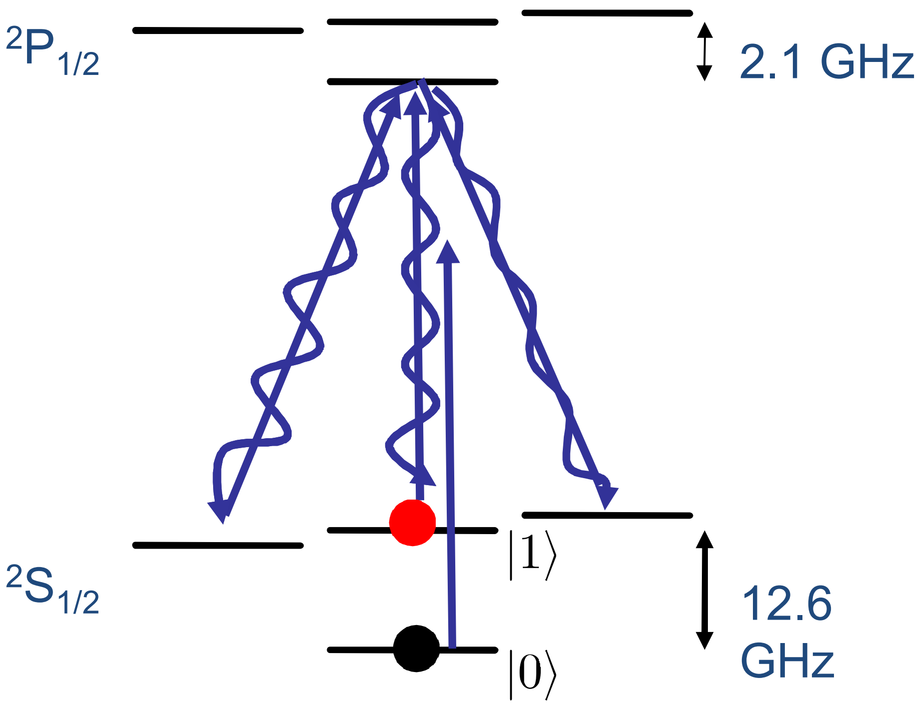

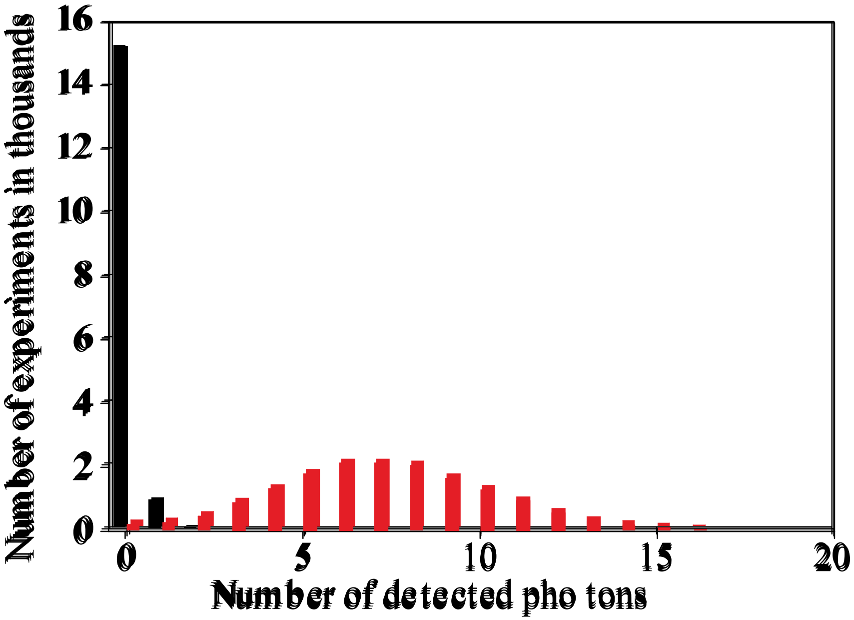

S. Olmschenk *et al.*, PRA **76**, 052314 (2007)

State detection for two ions

- Too much overlap between histograms of 1 and 2 bright ions
- Fit sums of experimentally measured 0, 1 and 2 ion bright histograms to determine probabilities of ensemble

Demonstration:

- Two trapped ions undergoing global Rabi oscillations
- Is described using one fit parameter: the π-time

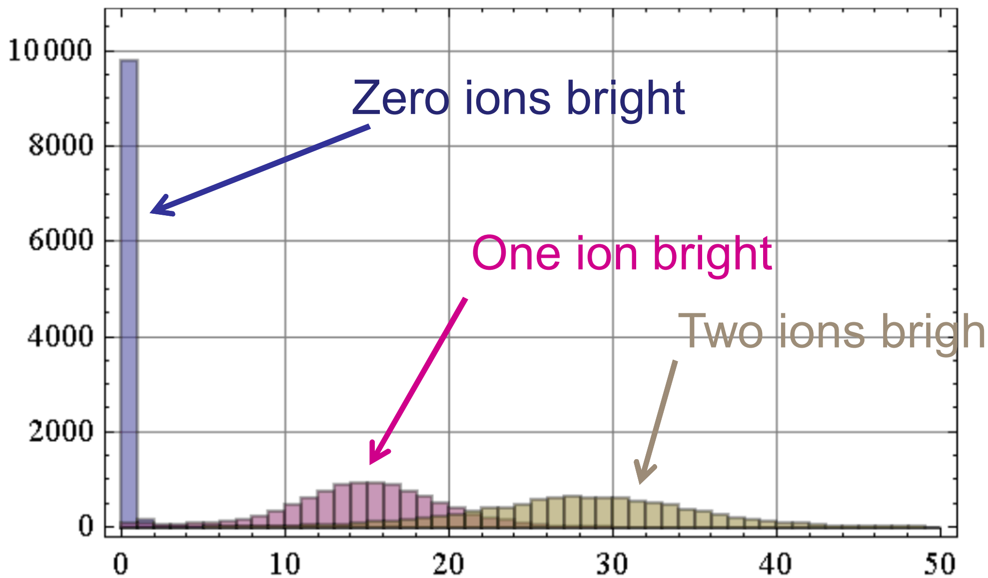

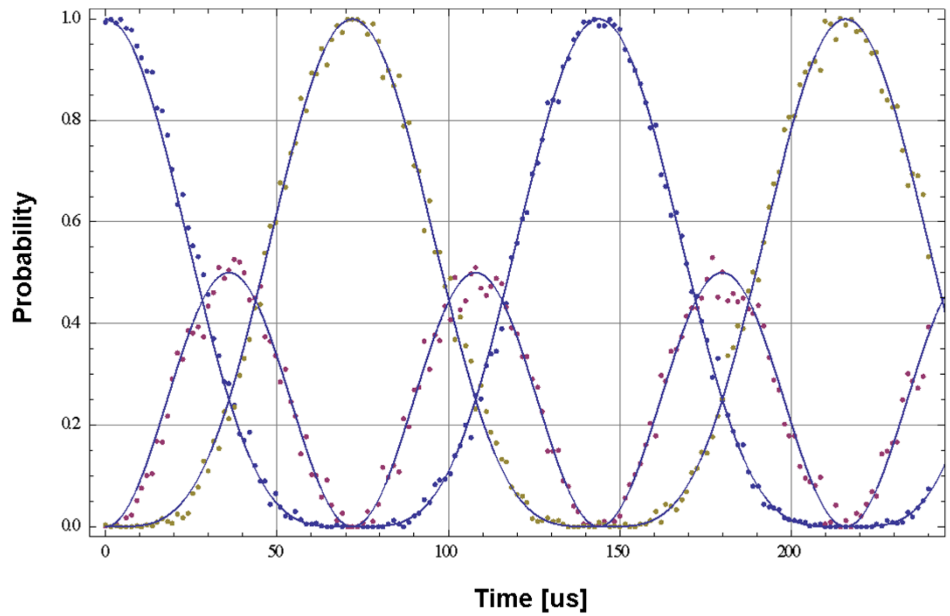

Sandia National Laboratories

HOA-2 trap

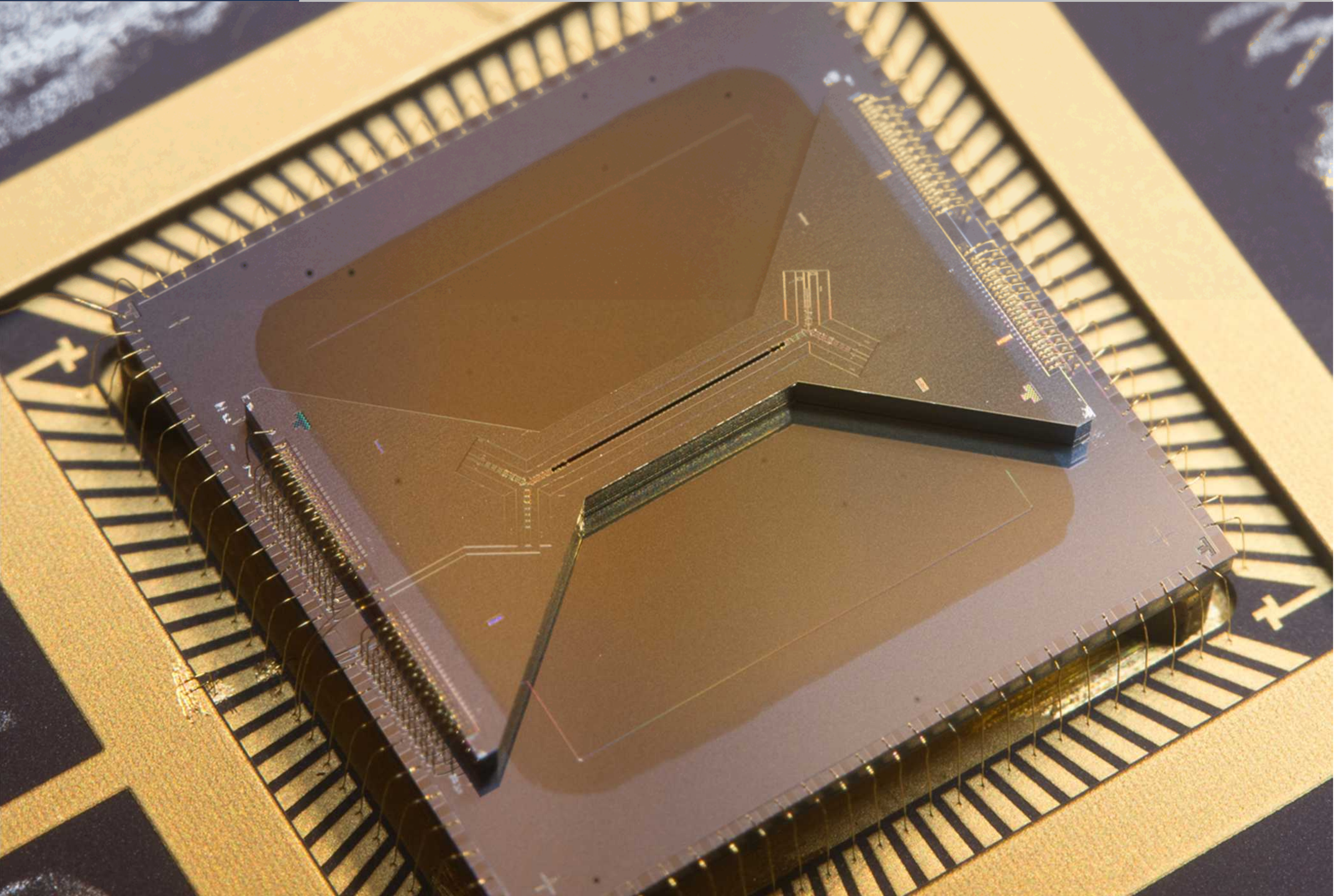

High Optical Access trap HOA-2

- Excellent optical access rivaling 3-D traps (NA 0.25 vertical, NA 0.12 lateral)
- High trap frequencies (small characteristic distance 140µm, closest electrode 90µm from ions)
- Full control over principal axes rotation (0 - 40 degree)
- Excellent axial control using segmented inner electrodes
  - Tighter and smaller axial trap
  - Much better separation and recombination of chains
- Small resistance between electrode and bondpad (<4Ω)
- Made possible by process improvements and optimizations

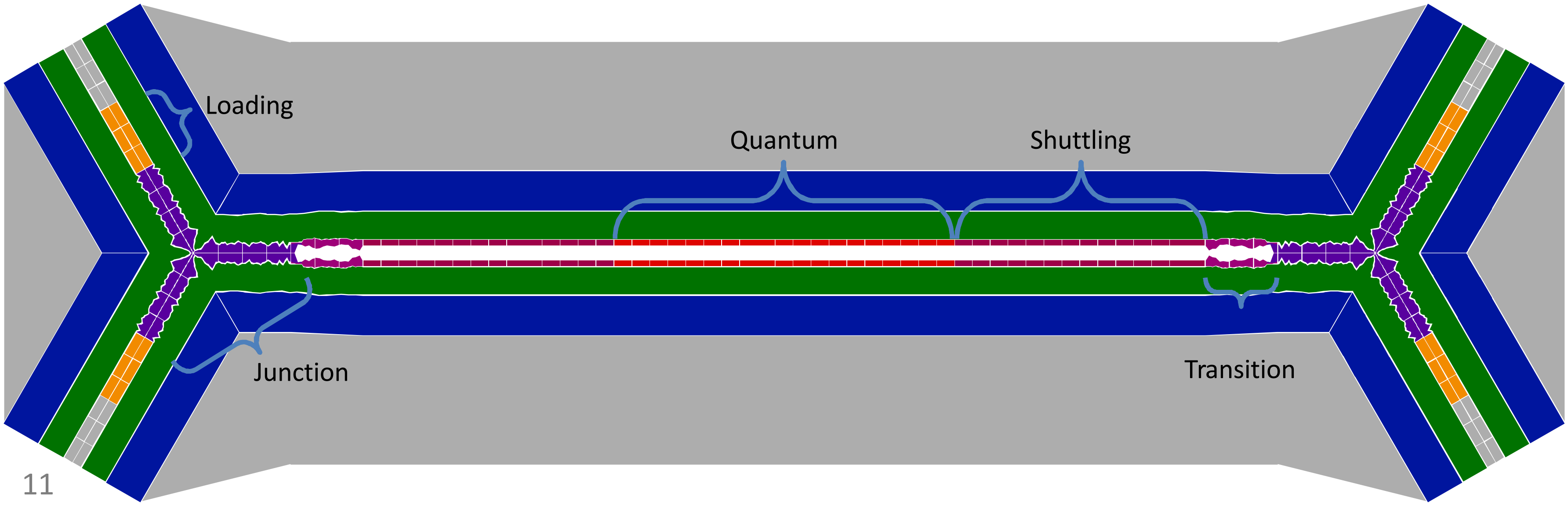

Trap details

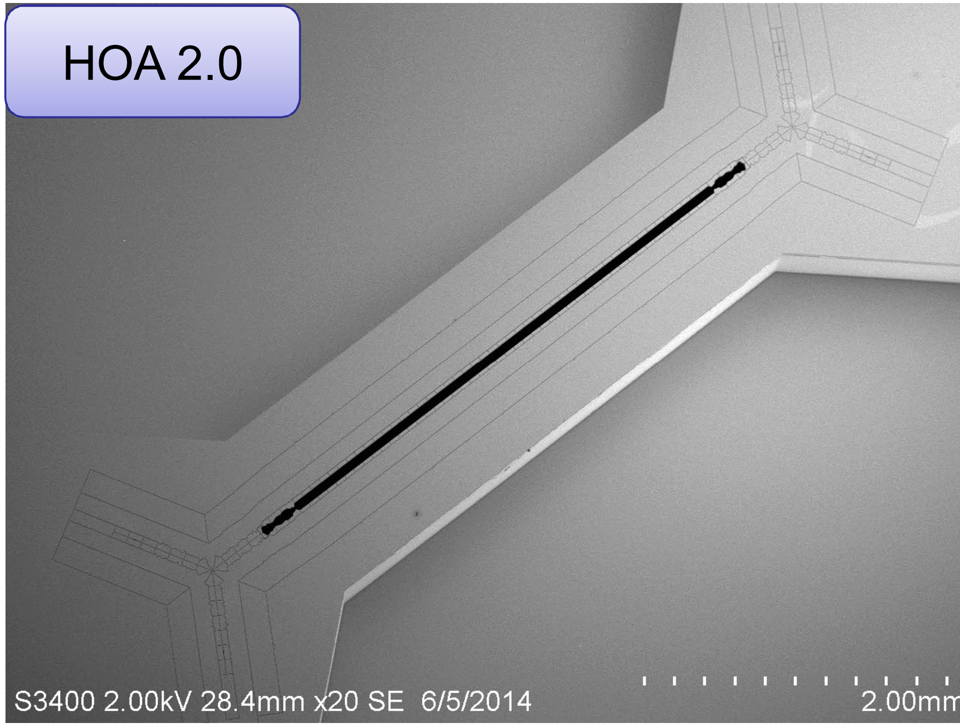

HOA 2.0

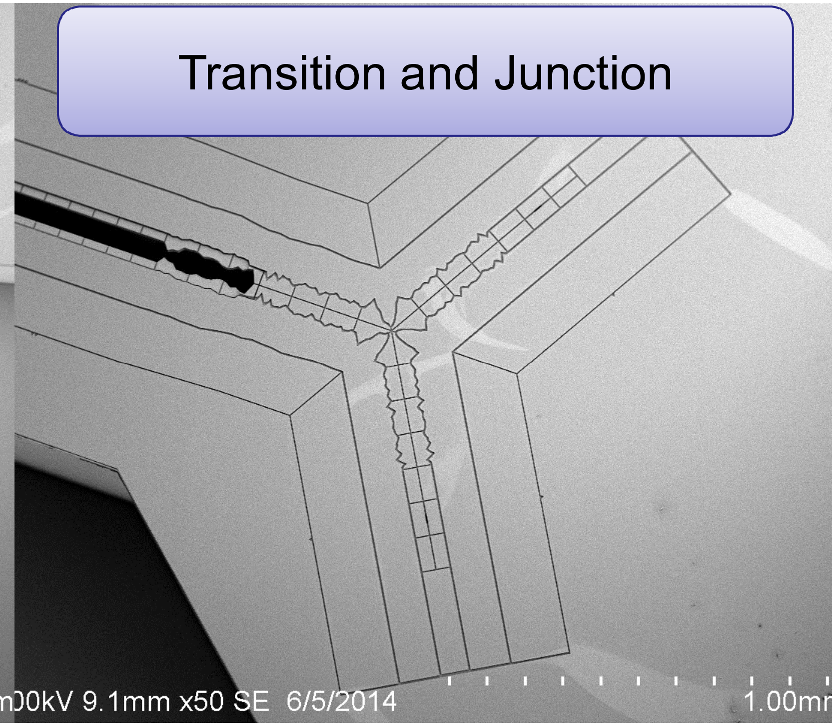

Transition and Junction

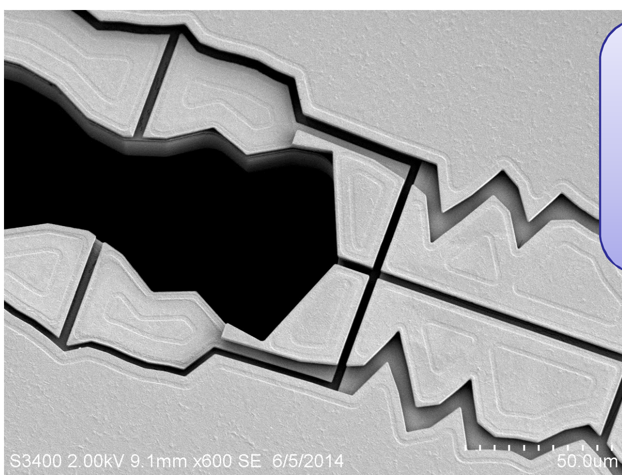

Vertical distance
12 µm

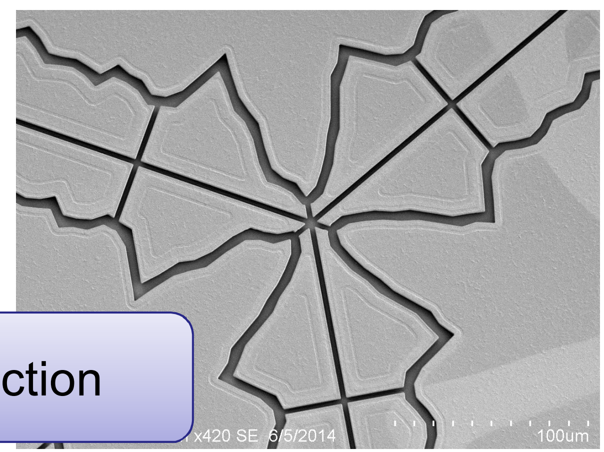

Junction

HOA-2 trap characteristics

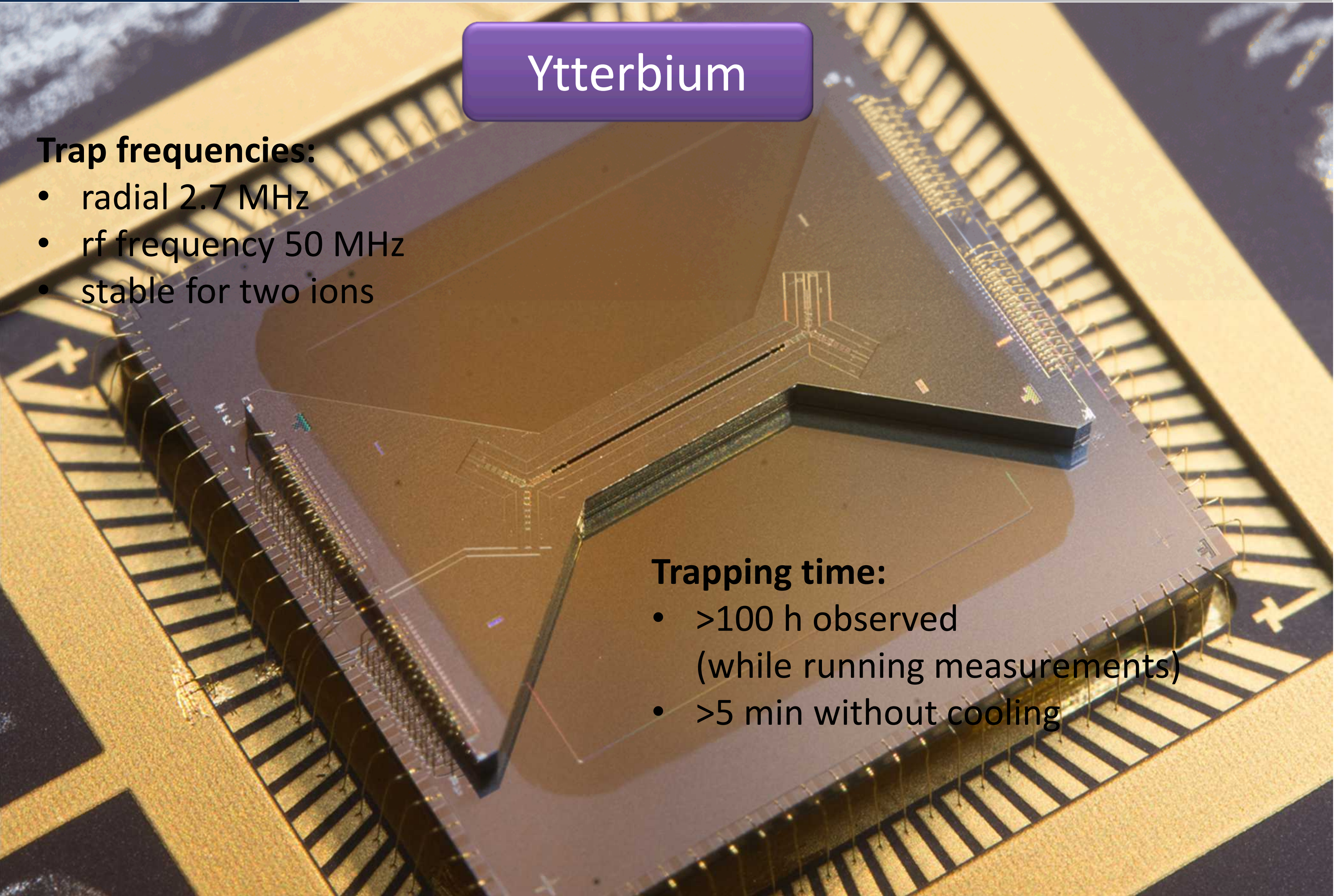

Ytterbium

Trap frequencies:

- radial 2.7 MHz
- rf frequency 50 MHz
- stable for two ions

Trapping time:

- >100 h observed
  (while running measurements)
- >5 min without cooling

HOA-2 heating rates

Heating rates as function of principal axes rotation

- Principal axes rotation measured by measuring π-times of Rabi flopping on cooled motional modes
- Minimal heating rates for motional mode parallel to trap surface $\dot{n}_{||}$
- Without technical noise: Vertical mode has at most $\dot{n}_{\perp} \leq 2\dot{n}_{||}$
  (P. Schindler, et al., Phys. Rev. A **92**, 013414 (2015).
- Limited by technical noise

$^{171}Yb^{+}$, Trap frequency 2.8 MHz, r.f. 50 MHz

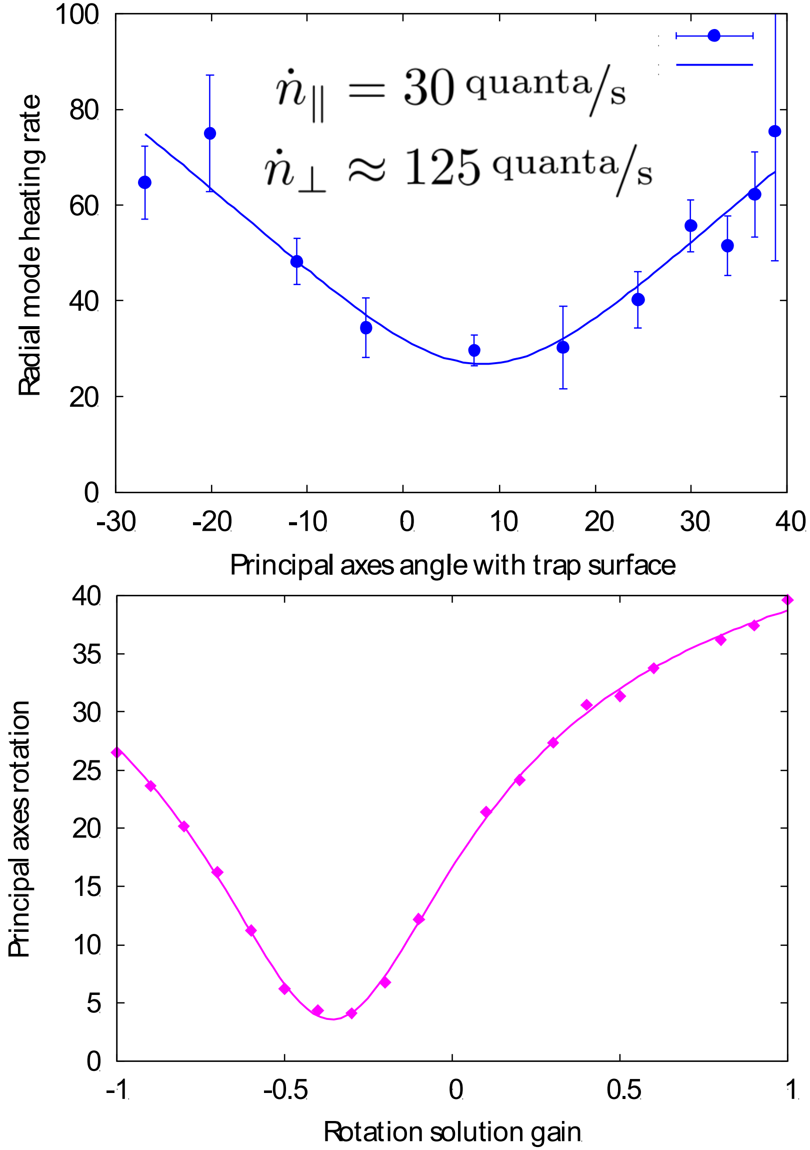

Sandia National Laboratories

Gate Set Tomography

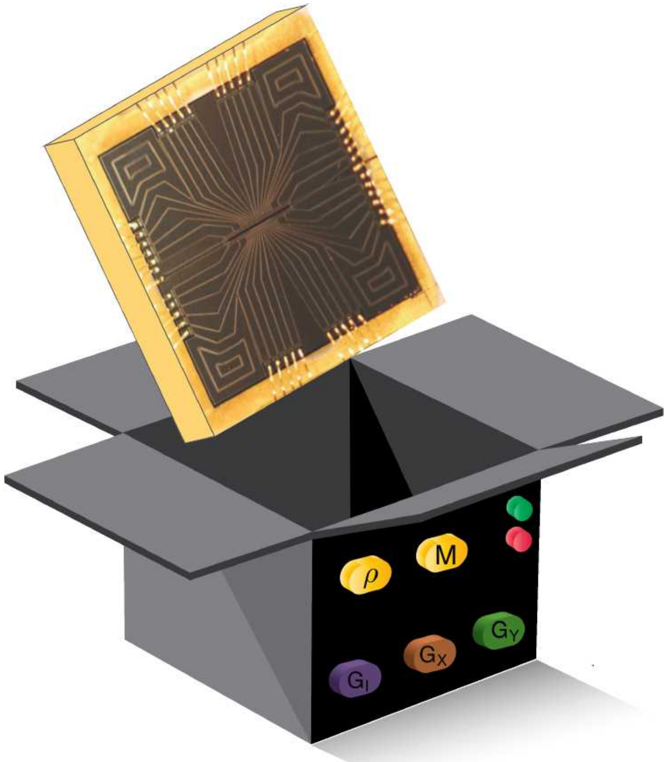

Developed at Sandia by
Robin Blume-Kohout et al. (1425)

- No calibration required
- Detailed debug information
- Efficiently measures performance characterizing fault-tolerance (diamond norm)
- Detects non-Markovian noise

Uses structured sequences to amplify all possible errors

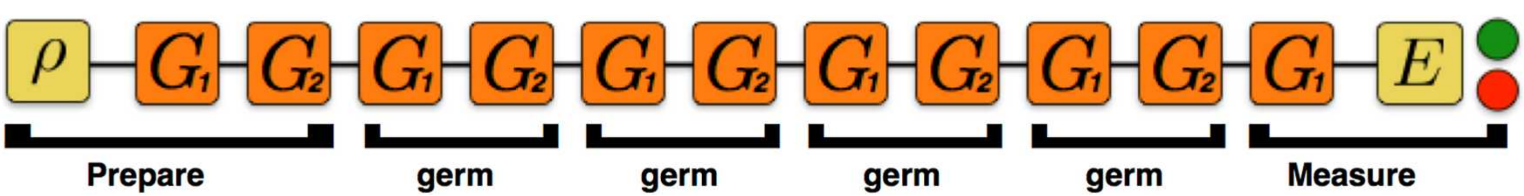

GST Experiments

Single qubit BB1 compensated microwave gates on $^{171}Yb^{+}$

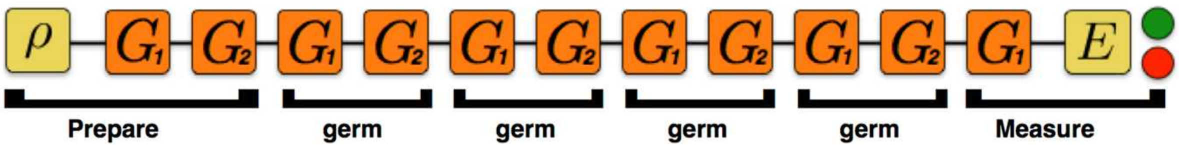

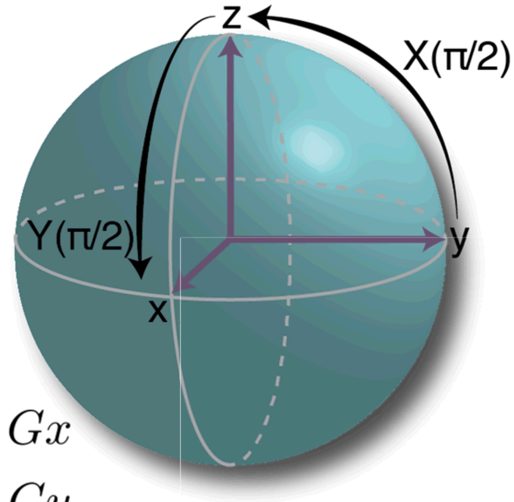

Desired "target" gates:

G_i Idle (Identity)

G_x $\pi/2$ rotation about x-axis

G_y $\pi/2$ rotation about y-axis

Fiducials:

$\{\}$

Gx

Gy

$Gx \cdot Gx$

$Gx \cdot Gx \cdot Gx$

$Gy \cdot Gy \cdot Gy$

Approximately prepare 6 points on Bloch sphere

Germs:

Gx

Gy

Gi

$Gx \cdot Gy$

$Gx \cdot Gy \cdot Gi$

$Gx \cdot Gi \cdot Gy$

$Gx \cdot Gi \cdot Gi$

$Gy \cdot Gi \cdot Gi$

$Gx \cdot Gx \cdot Gi \cdot Gy$

$Gx \cdot Gy \cdot Gy \cdot Gi$

$Gx \cdot Gx \cdot Gy \cdot Gx \cdot Gy \cdot Gy$

GST data

Raw data poor gates

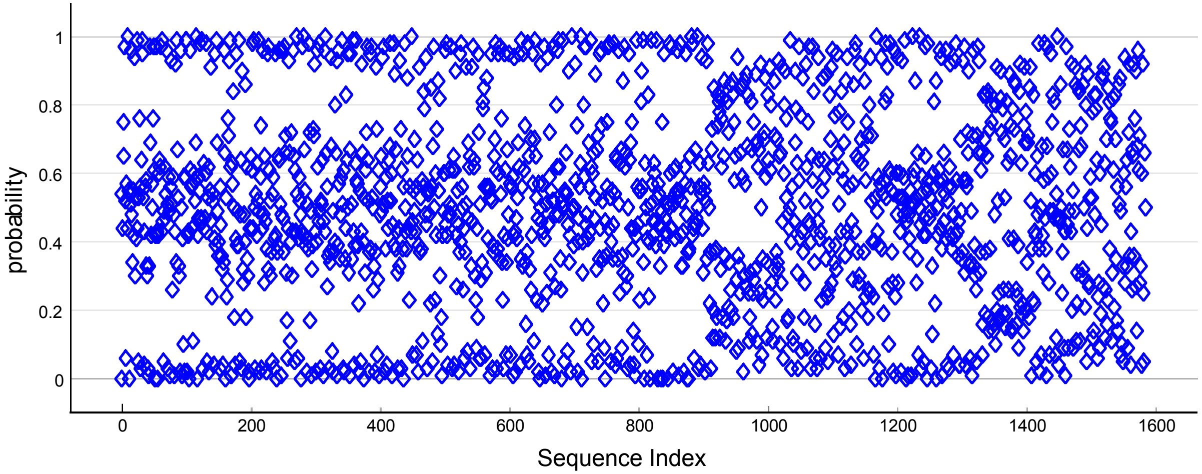

Raw data good gates

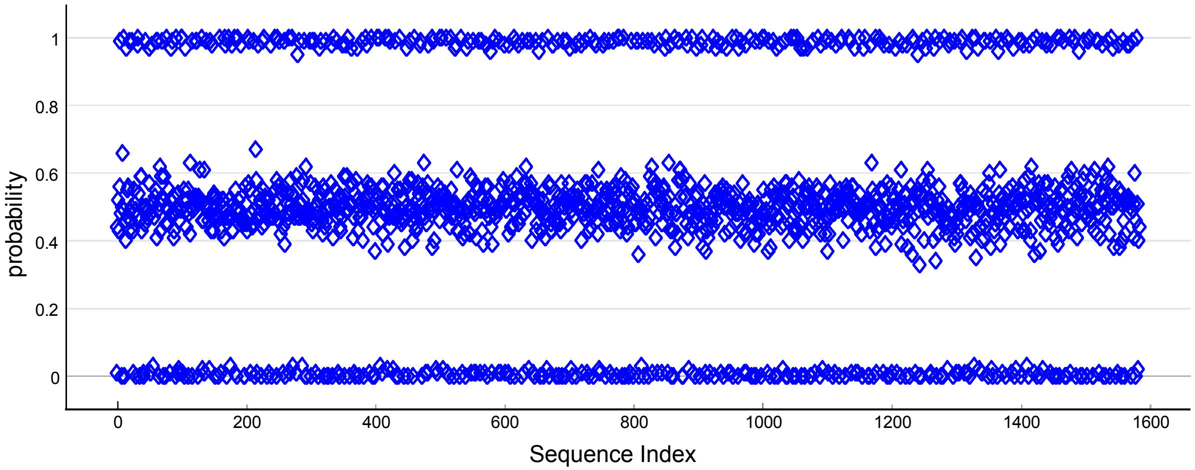

GST: debugging microwave gates

Gate	Rotn. axis	Angle
G_I	0.5252 -0.009 0.8506 -0.0244	0.001699π
G_X	-3×10^{-6} -1 -3×10^{-5} -0.009	0.501308π
G_Y	-0.2474 0.0001 0.9689 -0.0001	0.501366π

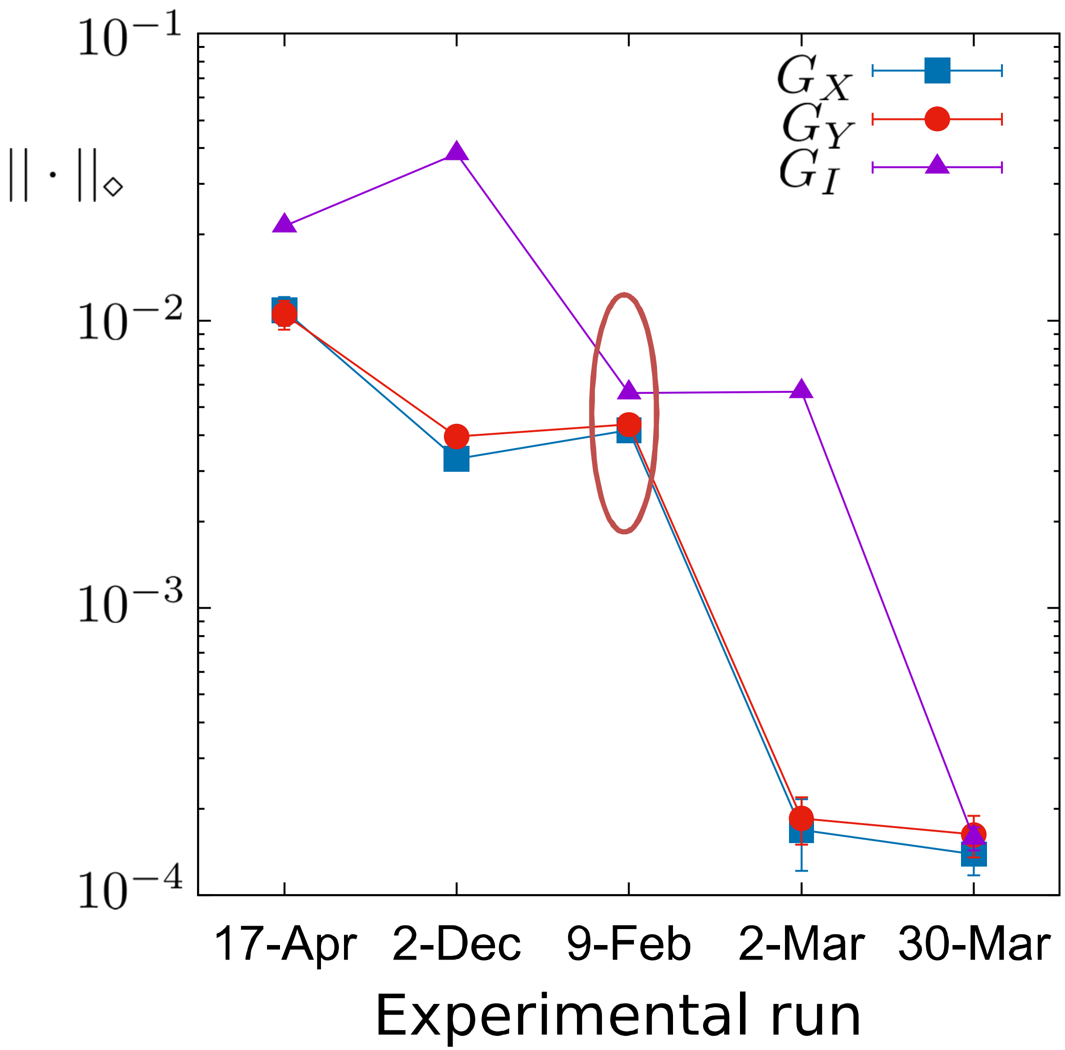

Broadband pulses

BB1 compensated pulse

Switching artifacts

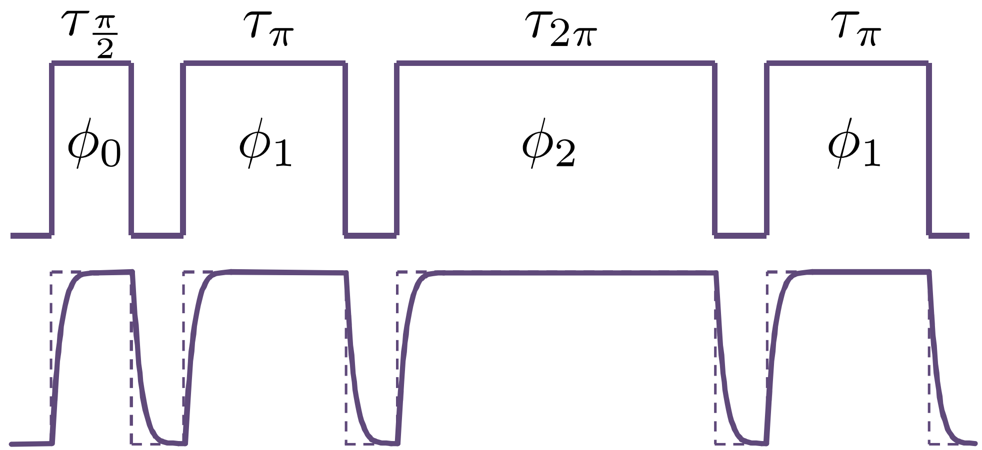

Example:

- Derivative vanishes at correct time
- However: Probability is *not* 50% as expected

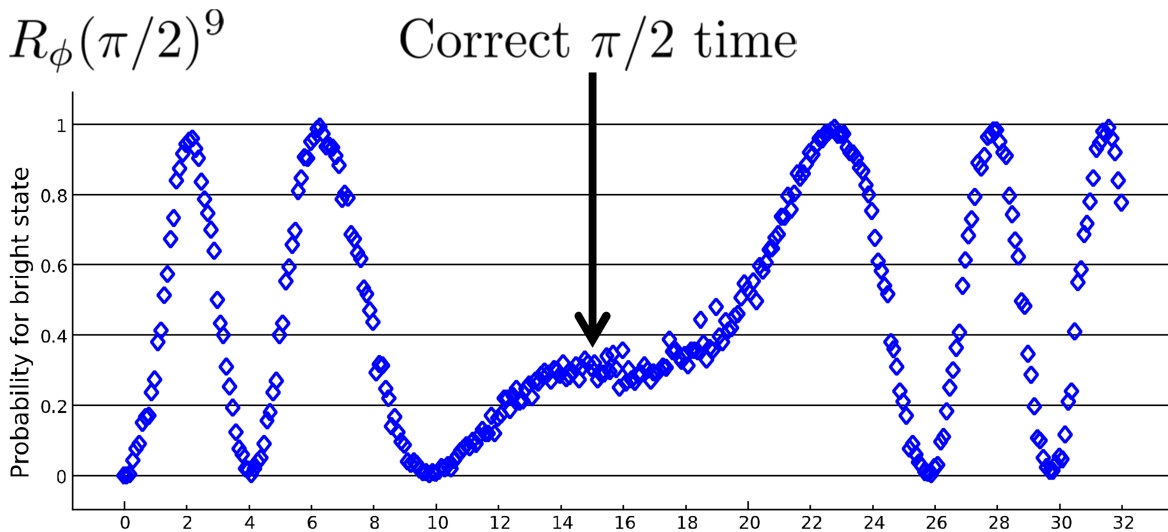

Broadband pulses

BB1 compensated pulse

Switching artefacts

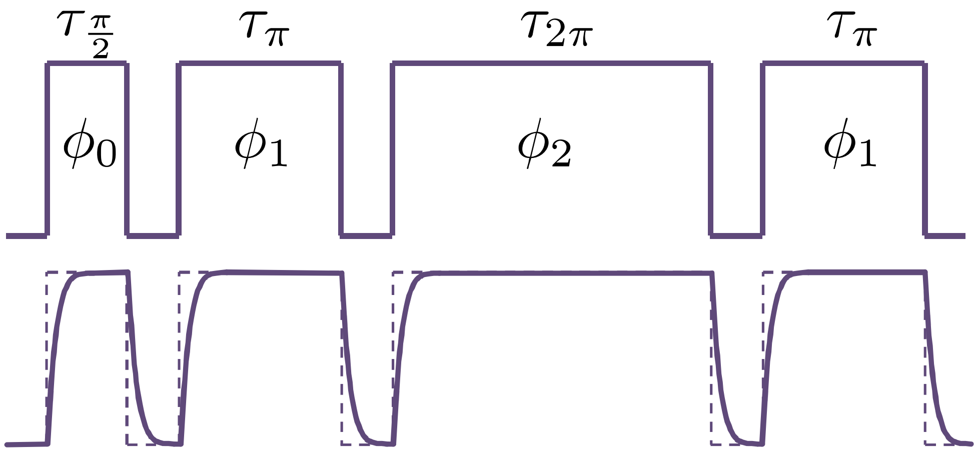

Calibration of offset time added to each pulse

$R_\phi(\pi/2)^{101}$

$R_\phi(\pi/2)^{103}$

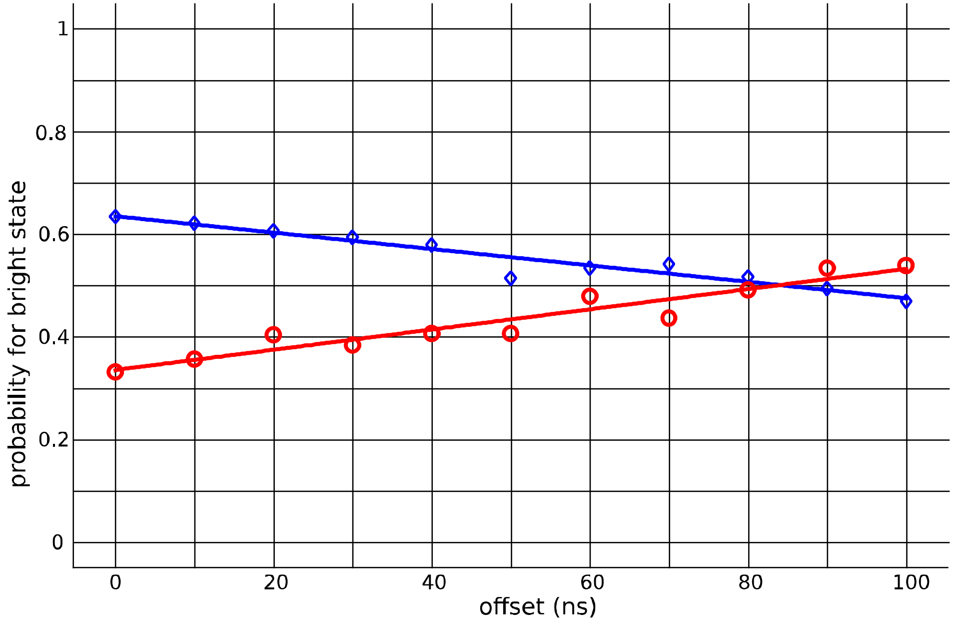

GST: debugging microwave gates

Gate	Rotn. axis	Angle
G_I	0.5252 -0.009 0.8506 -0.0244	0.001699π
G_X	-3×10^{-6} -1 -3×10^{-5} -0.009	0.501308π
G_Y	-0.2474 0.0001 0.9689 -0.0001	0.501366π

Gate	Rotn. axis	Angle
G_I	-0.0035 0.014 -0.9999 0.0006	0.001769π
G_X	-3×10^{-5} -1 1×10^{-4} 0.0006	0.500007π
G_Y	0.1104 4×10^{-5} 0.9939 0.0005	0.50001π

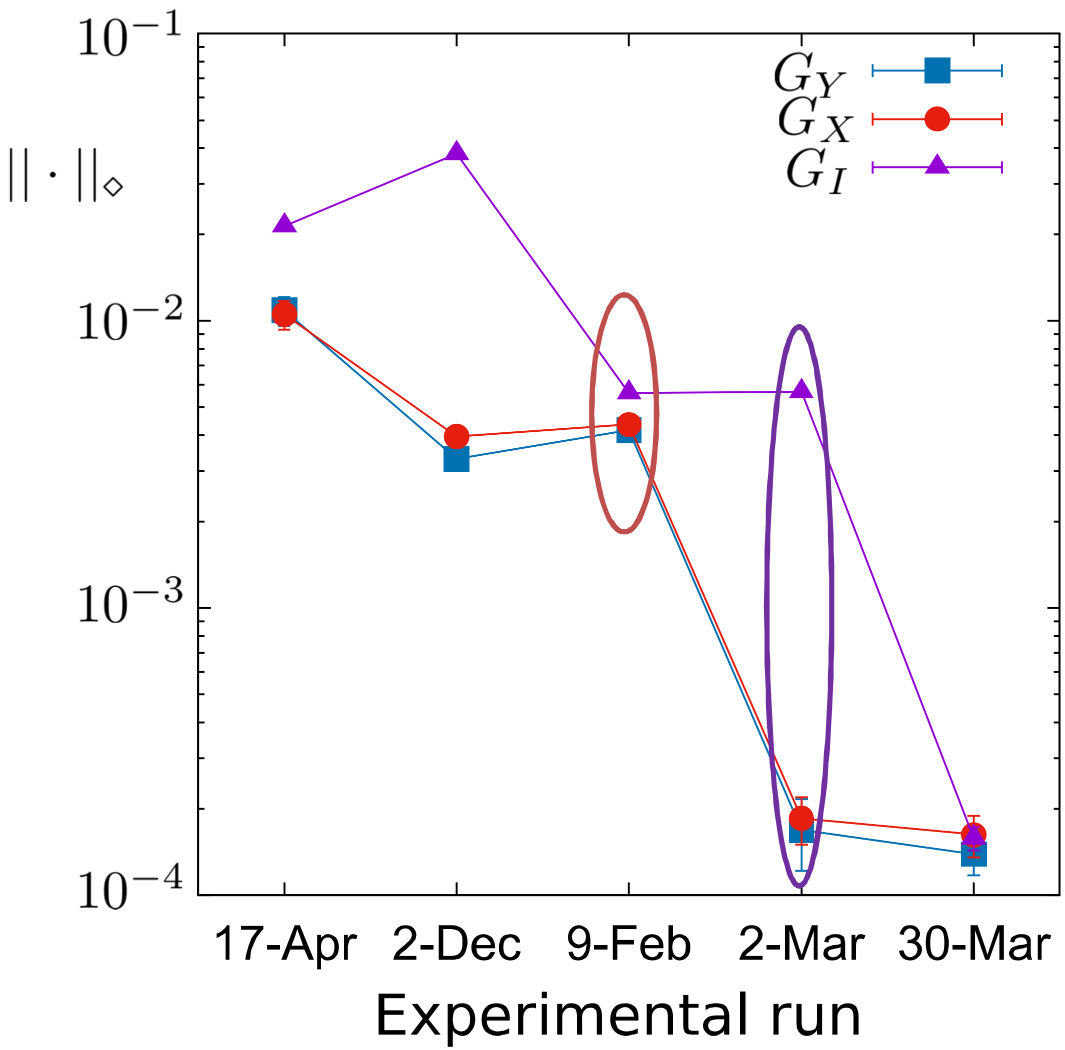

GST Markovianity violation microwave gates

The χ^2 values from the fits are expected to follow a χ^2 distribution with mean k and standard deviation $\sqrt{2k}$

$$\frac{\chi^2 - k}{\sqrt{2k}}$$

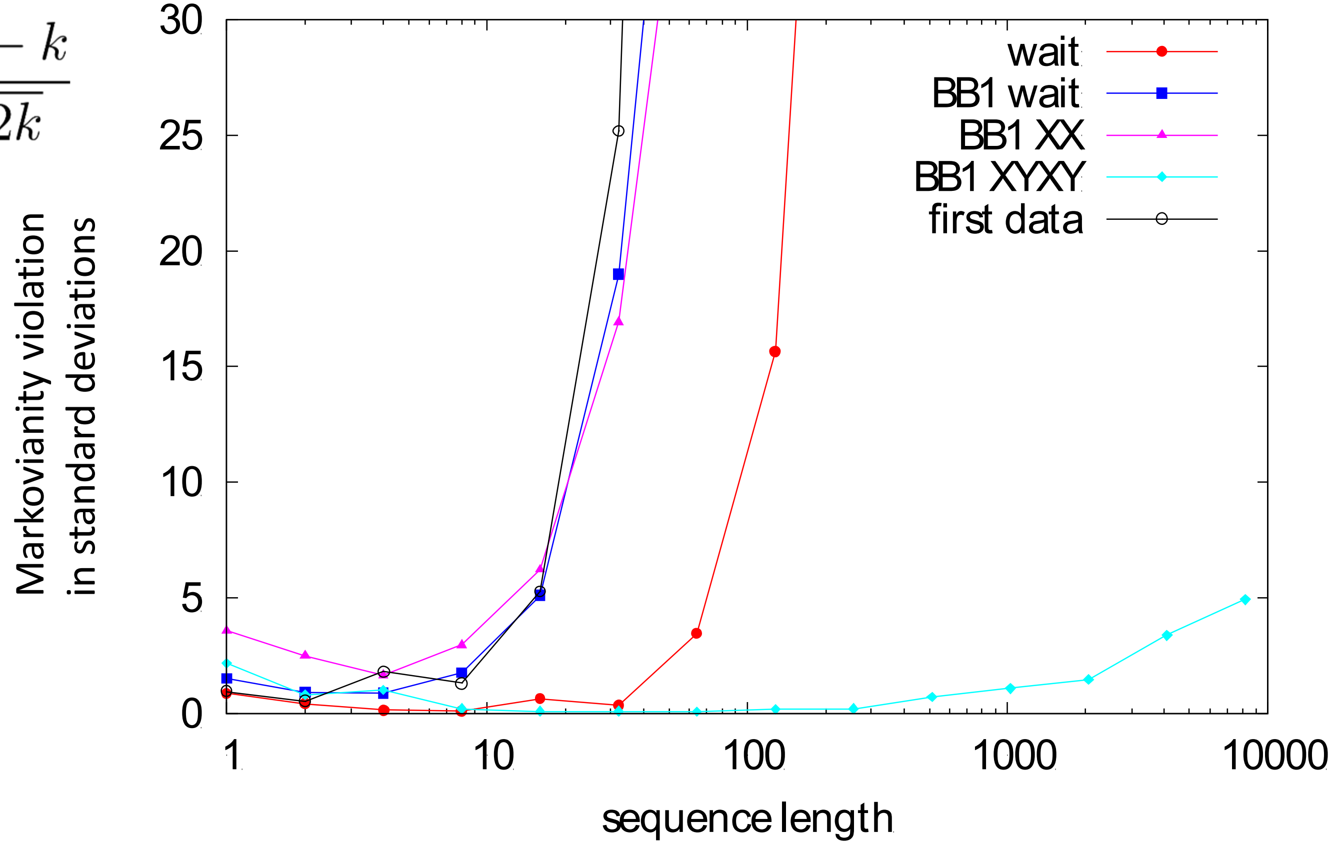

BB1 decoupled gates with decoupled identity have very small non-Markovian noise

GST: Microwave results

Best results for microwave single qubit gates:

- BB1 dynamically compensated pulse sequences
- Decoupling sequence for identity gate
- Drift control for π-time and qubit frequency

95% confidence intervals

Gate	Process Infidelity	$^1/_2$ $\diamond$-Norm
G_I	$6.9(6) \times 10^{-5}$	$7.9(7) \times 10^{-5}$
G_X	$6.1(7) \times 10^{-5}$	$7.0(15) \times 10^{-5}$
G_Y	$7.2(7) \times 10^{-5}$	$8.1(15) \times 10^{-5}$

All gates are better than the fault tolerance threshold of 9.7×10^{-5}
P. Aliferis and A. W. Cross, Phys. Rev. Lett. 98, 220502 (2007).

Possible limitations of microwave gates

- Time resolution:
  - Current time resolution is 5 ns
  - π-times are 45 μs
  - ratio: 10^{-4}
  - Possible due to broadband pulses
- Coherence time:
  - $T_2^* = 1\,\mathrm{s}$
  - longest pulse sequences $8192 : 1.66\,\mathrm{s}$

355 Raman transitions: $^{171}Yb^{+}$

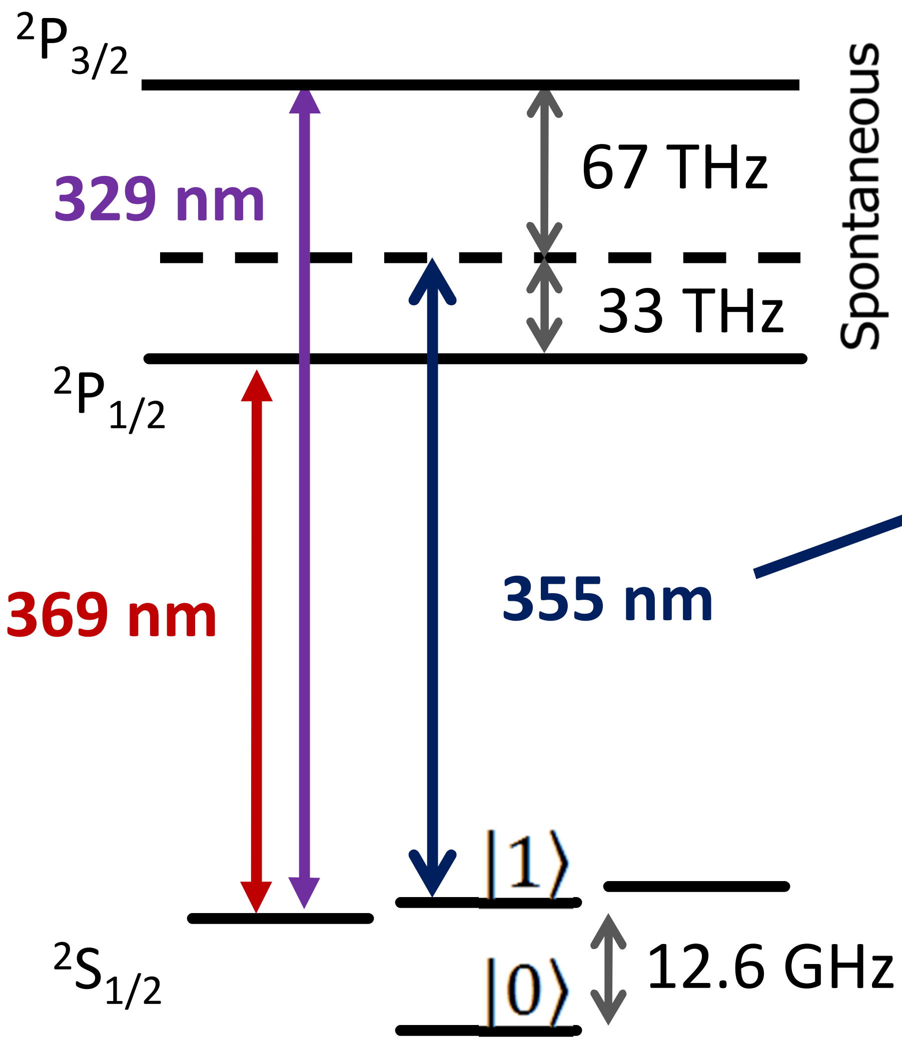

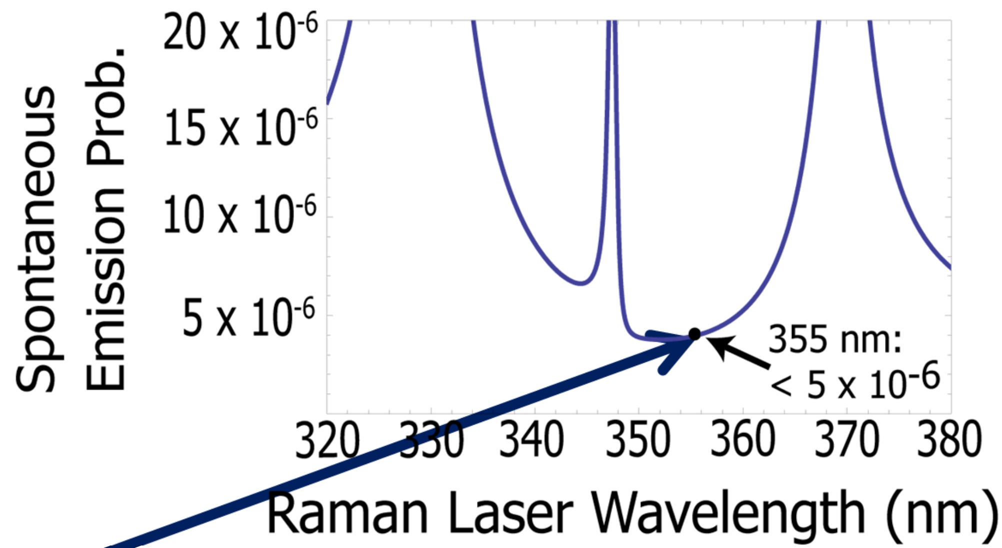

3x Nd:YVO_4 (355 nm) near minimum in Differential AC Stark Shift and spontaneous emission for $^{171}Yb^{+}$ ($\Delta_{Stark}/\Omega_{Rabi} < 3 \times 10^{-4}$ at 355 nm)

Pulsed laser Raman transitions

- Couple to ions using 355nm frequency comb
- Beat note created by repetition rate and AOM shift
- Get large splitting for free

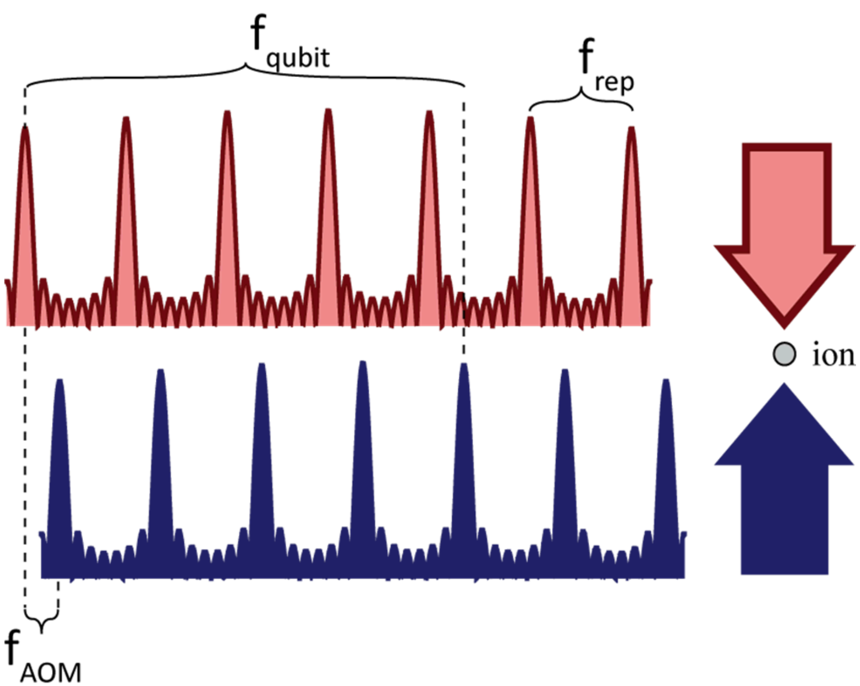

Requirement:

$$f_{qubit} = nf_{rep} \pm f_{AOM}$$

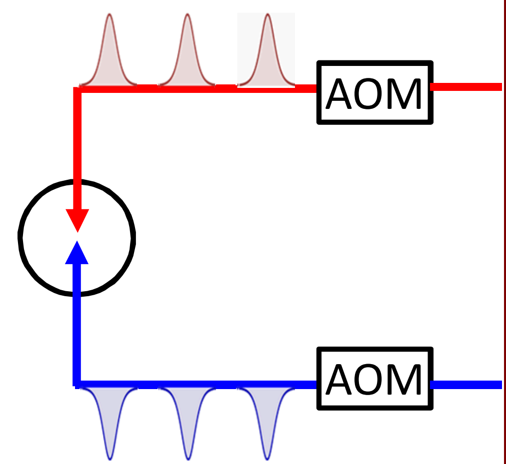

Stabilizing the beatnote frequency

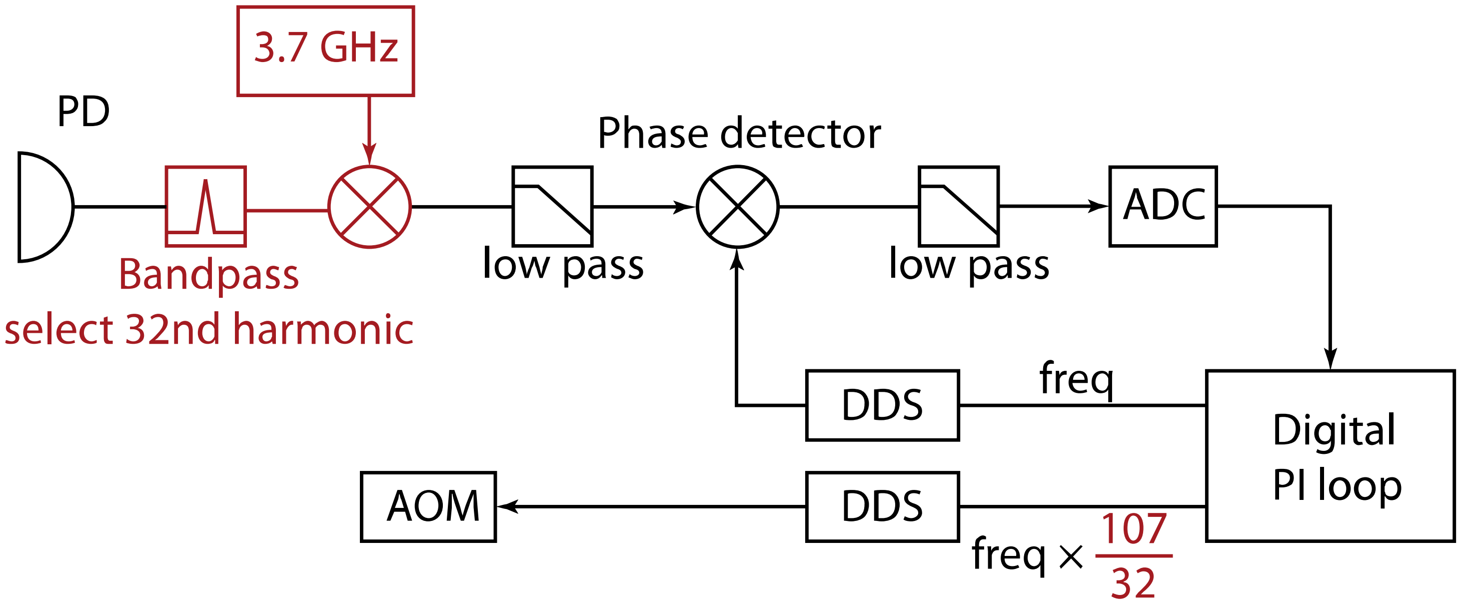

Sandia National Laboratories

“Gapless” Pulse Technique

BB1 compensated pulse

Finite turn-on time

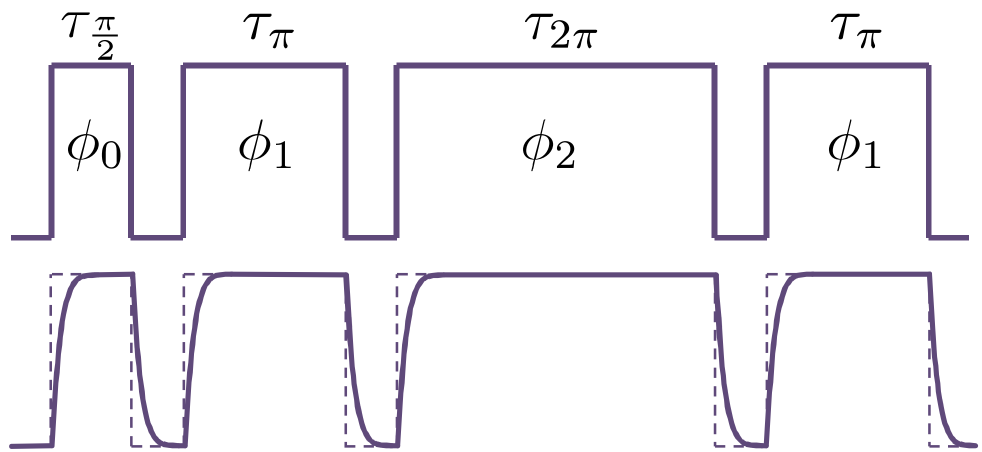

BB1 compensation assumes variations in pulse area are scaled proportionally for extra compensation pulses. Finite turn on-time effects are independent of pulse length and do not scale! Power stabilization of Raman beams is limited by ADC readout times in feedback loop.

Gapless pulse sequence

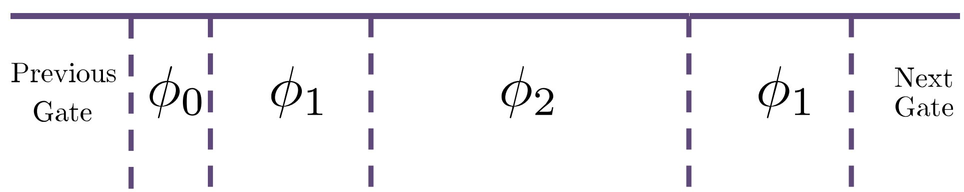

Discontinuous phase updates are used in place of gaps. Solves issues related to finite turn-on time and allows for continuous feedback on the driving field power.

GST: Raman laser results

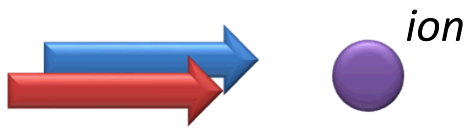

co-propagating beam geometry
- Motion independent
- No optical phase imprinted

- BB1 dynamically compensated pulse sequences

GST results:

95% confidence intervals

	Conventional pulses		Gapless pulses	
Gate	Process Infidelity	$1/2$ $\diamond$-Norm	Process Infidelity	$1/2$ $\diamond$-Norm
G_I	$0.05(2) \times 10^{-4}$	$12(1) \times 10^{-4}$	$1.1(1) \times 10^{-4}$	$5.3(2) \times 10^{-4}$
G_X	$1.3(1) \times 10^{-4}$	$4(2) \times 10^{-4}$	$0.5(1) \times 10^{-4}$	$2(6) \times 10^{-4}$
G_Y	$1.6(4) \times 10^{-4}$	$4(3) \times 10^{-4}$	$0.7(1) \times 10^{-4}$	$4(9) \times 10^{-4}$

Process Infidelity $< 1.2 \times 10^{-4}$

$1/2\diamond$-Norm $< 5.5 \times 10^{-4}$

Markovianity violation

Gapless versus standard pulses

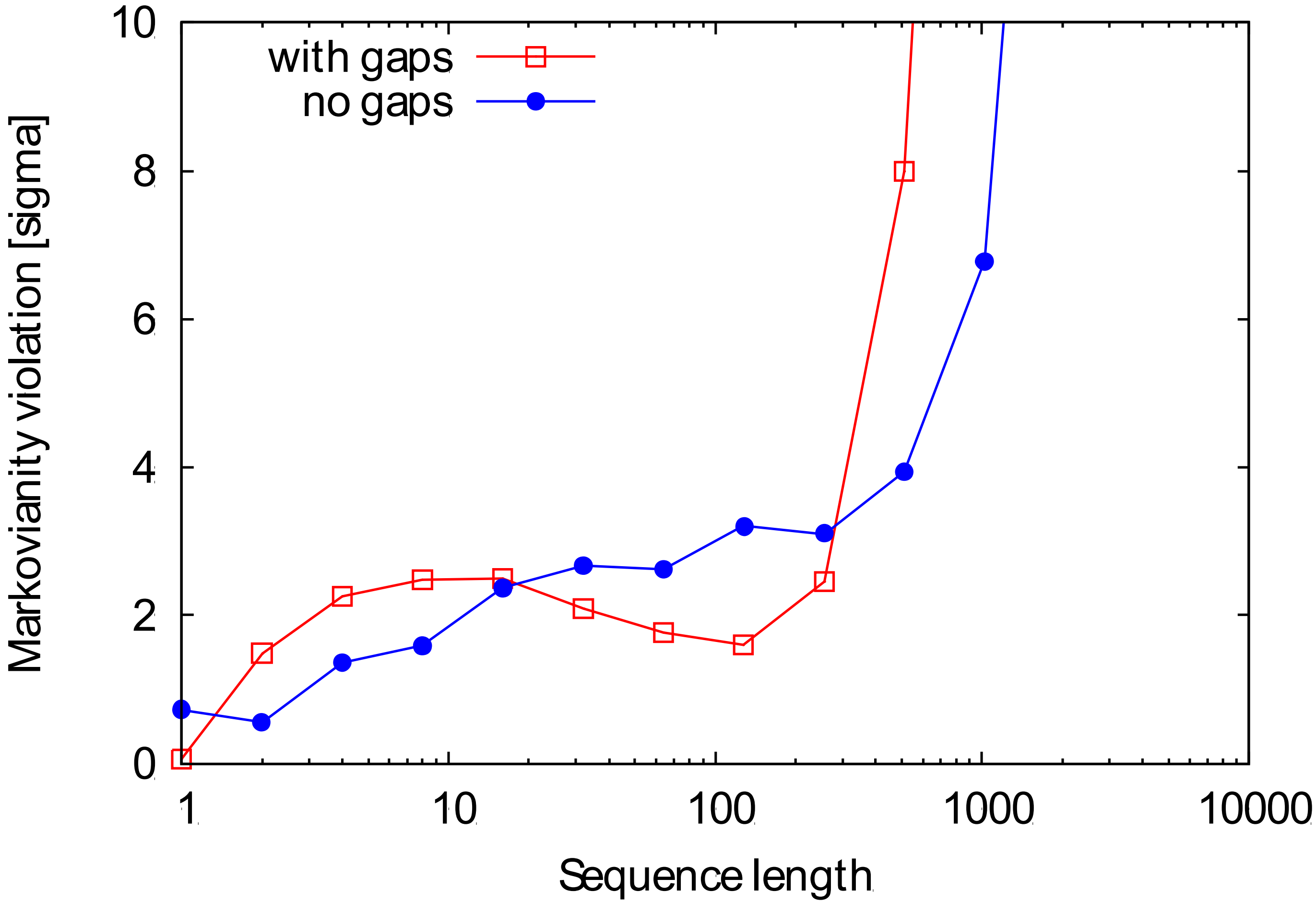

GST: Raman laser results

counter-propagating beam geometry

- Motion can be addressed
- Imprints an optical phase on the qubit

- BB1 dynamically compensated pulse sequences

95% confidence intervals

	Compensated identity		Wait identity	
Gate	Process Infidelity	$1/2$ $\diamond$-Norm	Process Infidelity	$1/2$ $\diamond$-Norm
G_I	$11(1) \times 10^{-4}$	$23(1) \times 10^{-4}$	$0.9(2) \times 10^{-4}$	$8.8(4) \times 10^{-4}$
G_X	$3.9(4) \times 10^{-4}$	$13(6) \times 10^{-4}$	$5.8(4) \times 10^{-4}$	$15(6) \times 10^{-4}$
G_Y	$4.1(4) \times 10^{-4}$	$8(8) \times 10^{-4}$	$5.8(4) \times 10^{-4}$	$9(11) \times 10^{-4}$

$$\text{Process Infidelity} < 6.2 \times 10^{-4}$$
$$1/2\,\diamond\text{-Norm} < 21 \times 10^{-4}$$

Two-qubit gate implementation

Sandia National Laboratories

- Mølmer-Sørensen gates [1]
- All two-qubit gates implemented using Walsh compensation pulses [2]

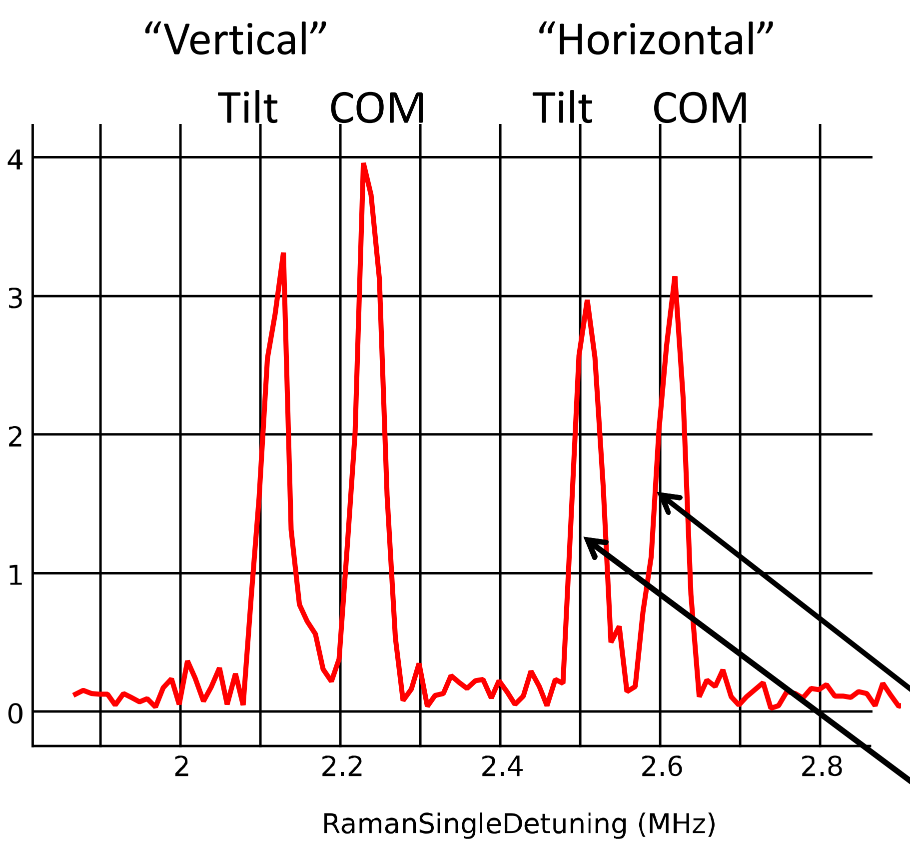

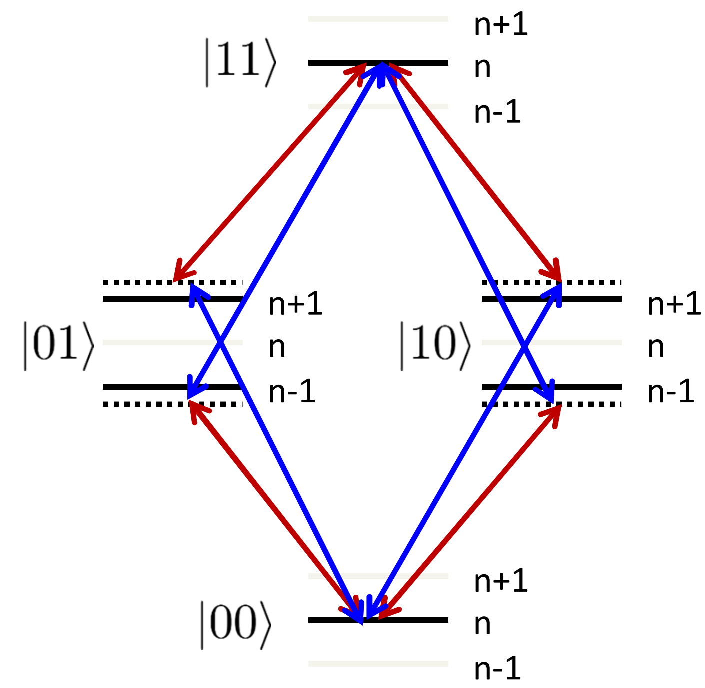

$|00\rangle \rightarrow |00\rangle + |11\rangle$

Heating rates

$\approx 60\ ^{\text{quanta}}/_{\text{s}}$

$< 8\ ^{\text{quanta}}/_{\text{s}}$

[1] K. Mølmer, A. Sørensen, PRL 82, 1835 (1999)
[2] D. Hayes et al. Phys. Rev. Lett. 109, 020503 (2012)

Two-qubit gate implementation

- Implemented using Walsh compensation pulses
- Optical phase sensitive

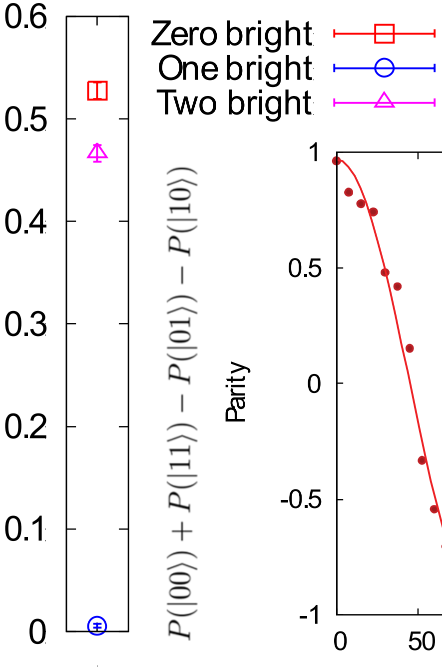

Data from February 12, 2015

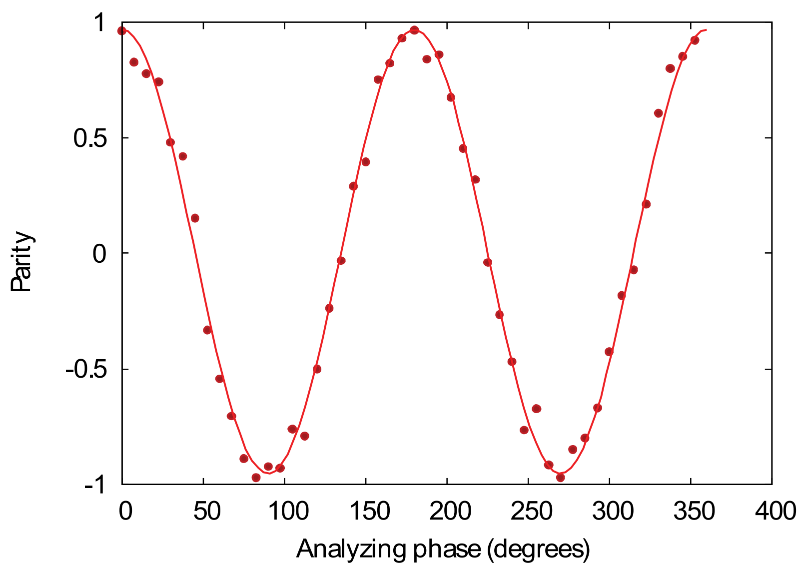

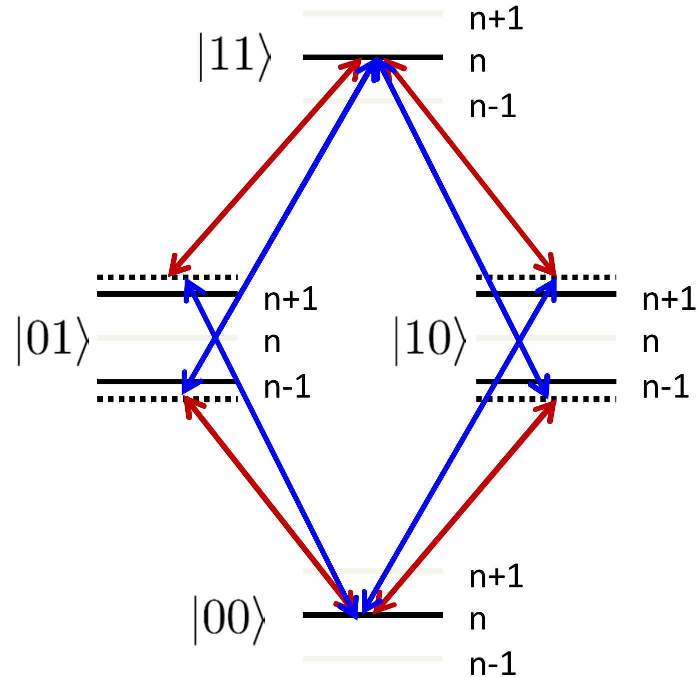

$$|00\rangle \rightarrow |00\rangle + |11\rangle$$

$$\mathcal{F} = \frac{1}{2}(P(|00\rangle) + P(|11\rangle)) + \frac{1}{4}c = 0.977$$

Data from February 12, 2015

Two-qubit gate implementation

- Implemented using Walsh compensation pulses
- Optical phase sensitive

Data from October 10, 2015

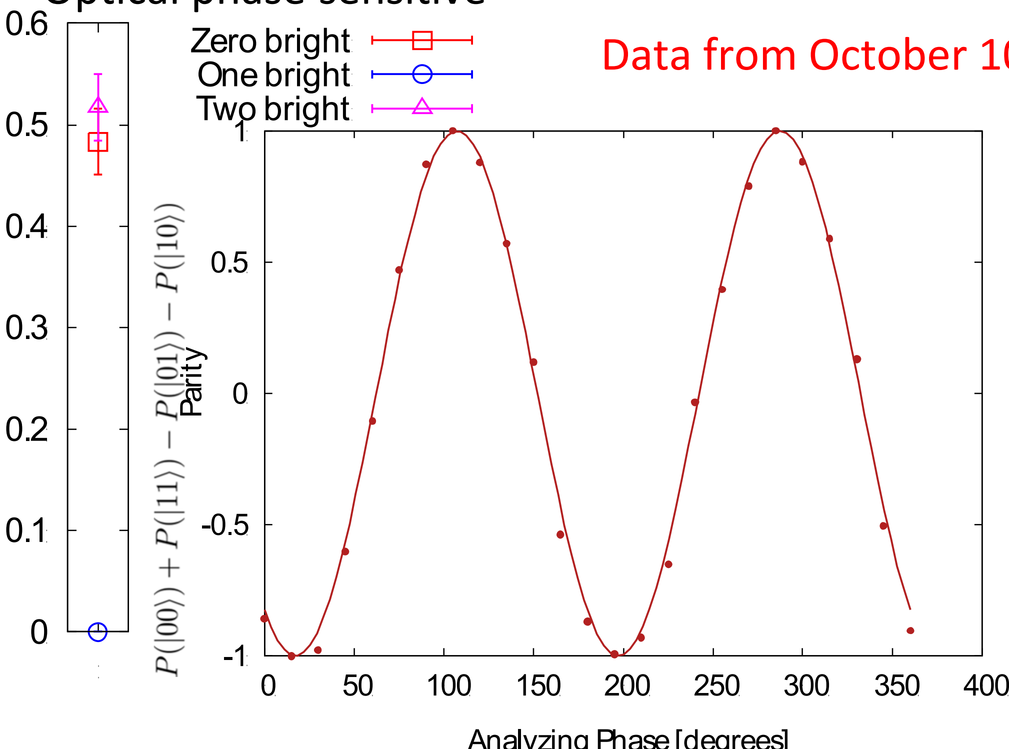

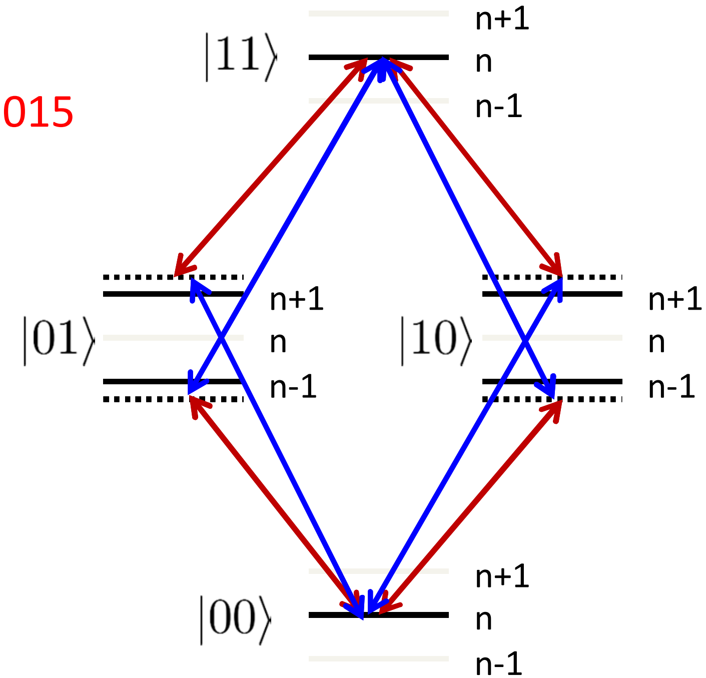

$$|00\rangle \rightarrow |00\rangle + |11\rangle$$

$$\mathcal{F} = \frac{1}{2}(P(|00\rangle) + P(|11\rangle)) + \frac{1}{4}c = 0.977$$

Data from February 12, 2015

$$\mathcal{F} = \frac{1}{2}(P(|00\rangle) + P(|11\rangle)) + \frac{1}{4}c \approx 0.995$$

Data from October 10, 2015

Process fidelity of two-qubit gate

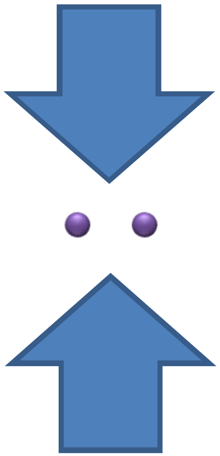

Currently:
- Two ions in single trap well
- No individual addressing

- Ideally all operations are symmetric
- Only symmetric subspace of two-qubit Hilbert space is accessible

Solution:
Perform GST on symmetric subspace
of two-qubit Hilbert space

Fundamental gates:

$$G_I$$

$$G_{XX} = G_X \otimes G_X$$

$$G_{YY} = G_Y \otimes G_Y$$

$$G_{MS}$$

9 Preparation Fiducials
12 Germs
6 Measurement Fiducials:

GST on symmetric subspace

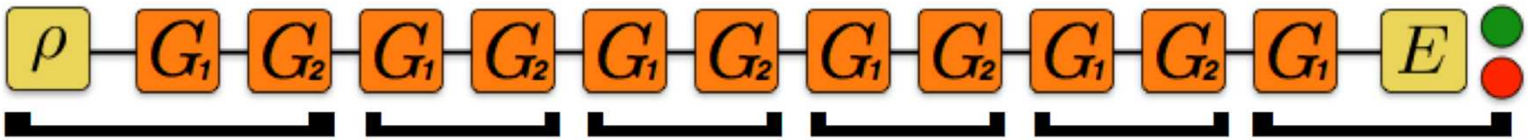

Basic gates:

$$G_I$$

$$G_{XX} = G_X \otimes G_X$$

$$G_{YY} = G_Y \otimes G_Y$$

$$G_{MS}$$

Preparation Fiducials:

$\{\}$

G_{XX}

G_{YY}

G_{MS}

$G_{XX}G_{MS}$

$G_{YY}G_{MS}$

Germs:

G_I

G_{XX}

G_{YY}

G_{MS}

$G_I G_{XX}$

$G_I G_{YY}$

$G_I G_{MS}$

$G_{XX} G_{YY}$

$G_{XX} G_{MS}$

$G_{YY} G_{MS}$

$G_I G_I G_{XX}$

$G_I G_I G_{YY}$

Detection Fiducials:

$\{\}$

G_{XX}

G_{YY}

G_{MS}

$G_{XX}G_{MS}$

$G_{YY}G_{MS}$

G_{XX}^3

G_{YY}^3

$G_{YY}^2 G_{MS}$

Two qubit GST raw data

GST; poor gate performance

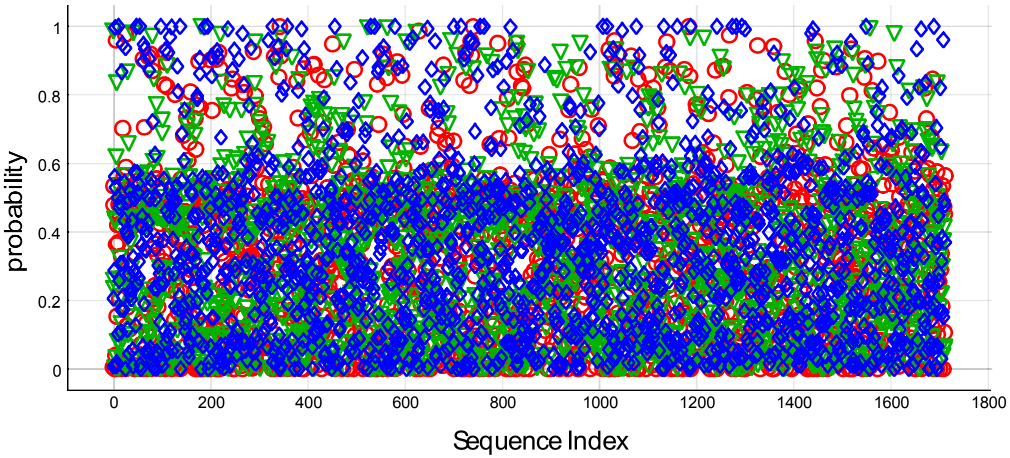

GST; good gate performance

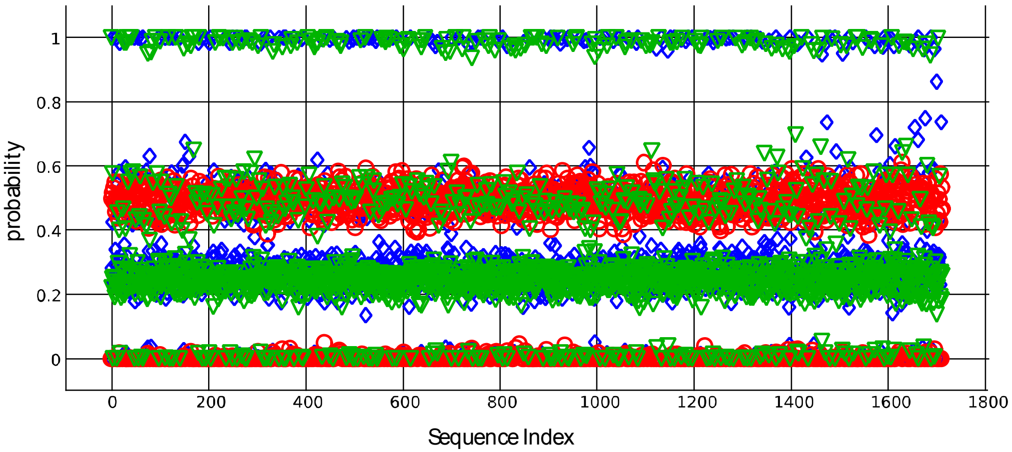

Zero ions bright

One ion bright

Two ions bright

Two qubit gate characterization

Gate	Process infidelity	$\frac{1}{2}$ Diamond norm
G_I	$1.6 \times 10^{-3} \pm 1.6 \times 10^{-3}$	$28 \times 10^{-3} \pm 7 \times 10^{-3}$
G_{XX}	$0.4 \times 10^{-3} \pm 1.0 \times 10^{-3}$	$27 \times 10^{-3} \pm 5 \times 10^{-3}$
G_{YY}	$0.1 \times 10^{-3} \pm 0.9 \times 10^{-3}$	$26 \times 10^{-3} \pm 4 \times 10^{-3}$
G_{MS}	$4.2 \times 10^{-3} \pm 0.6 \times 10^{-3}$	$38 \times 10^{-3} \pm 5 \times 10^{-3}$

95% confidence intervals

Process fidelity of two-qubit Mølmer-Sørensen gate > 99.5%

The best characterized two qubit gate

By the way: It's in a scalable surface trap

Sandia National Laboratories

Conclusion

Sandia microfabricated surface traps are ready for your high fidelity operations

Demonstrated:

- Long lifetime, observed ion > 100h
- High fidelity microwave single qubit gates
  Process infidelity $7.2(7) \times 10^{-5}$
  below fault tolerance threshold $\frac{1}{2} \|\cdot\|_\diamond = 8(1) \times 10^{-5}$
- High fidelity Raman laser single qubit gates
  Process infidelity 1.6×10^{-4} $\frac{1}{2} \|\cdot\|_\diamond = 5.3(2) \times 10^{-4}$
- High fidelity two qubit gates
  Process infidelity $4.2(6) \times 10^{-3}$ $\frac{1}{2} \|\cdot\|_\diamond = 38(5) \times 10^{-3}$

Thanks

Peter Maunz, Robin Blume-Kohout, M. G. Blain, C. Clark, S. Clark, K. Fortier, R. Haltli, E. Heller, A. Hollowell, D. Lobser, J. Mizrahi, E. Nielsen, P. Resnick, J. Rembetski, K. Rudinger, J. D. Sterk, D. L. Stick, C. Tigges, J. Van Der Wall.

Pulsed laser Raman transitions

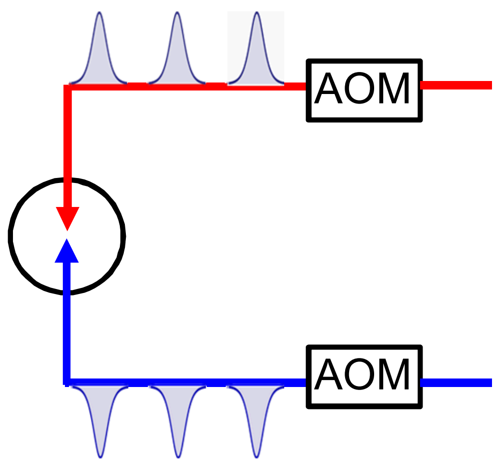

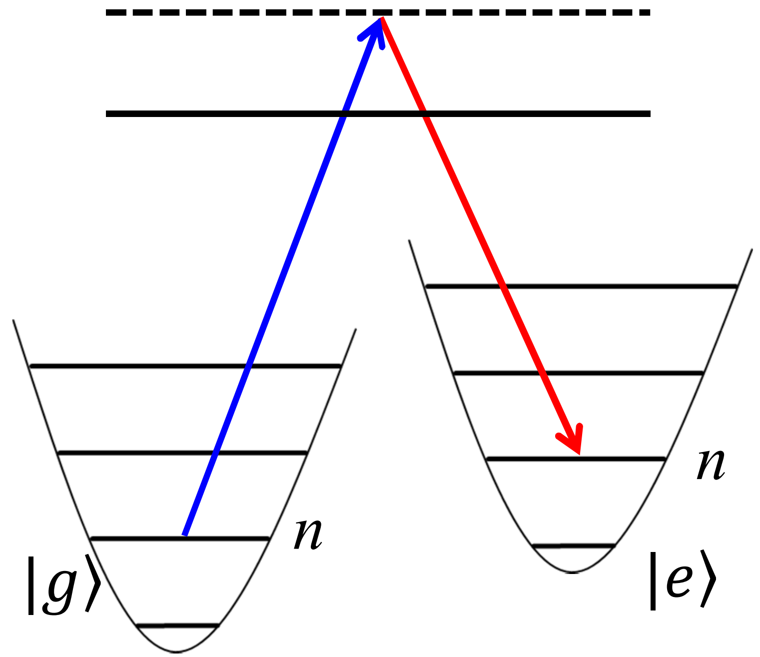

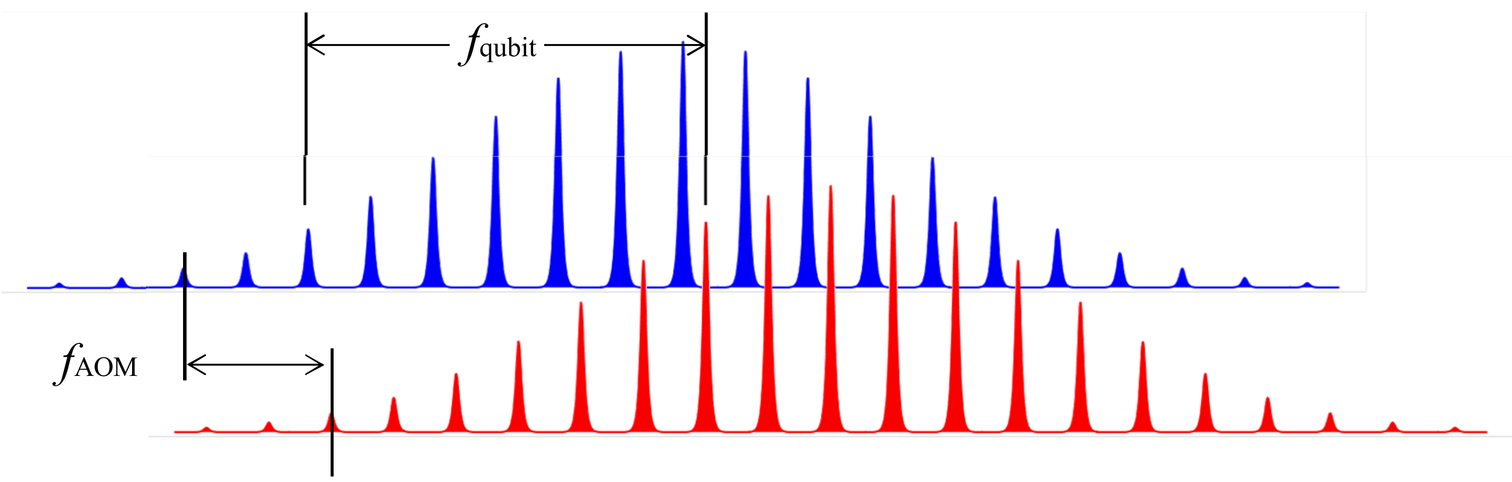

Towards scalable ion traps

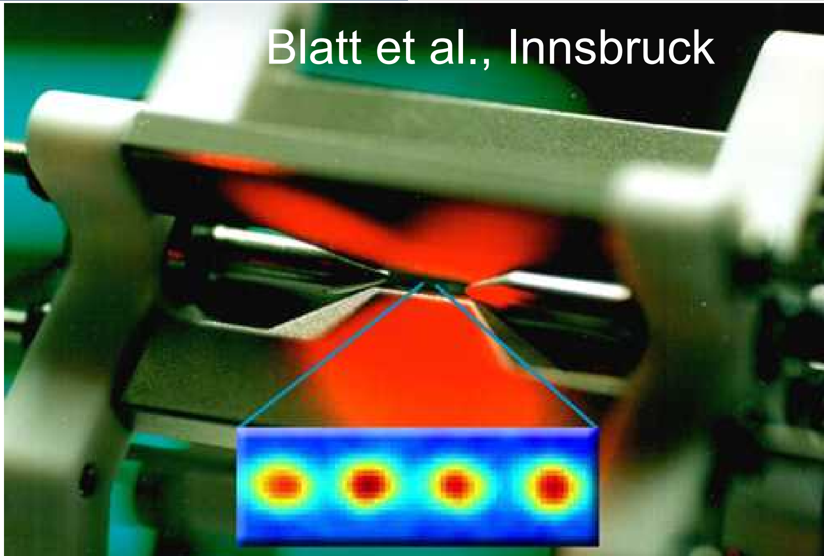

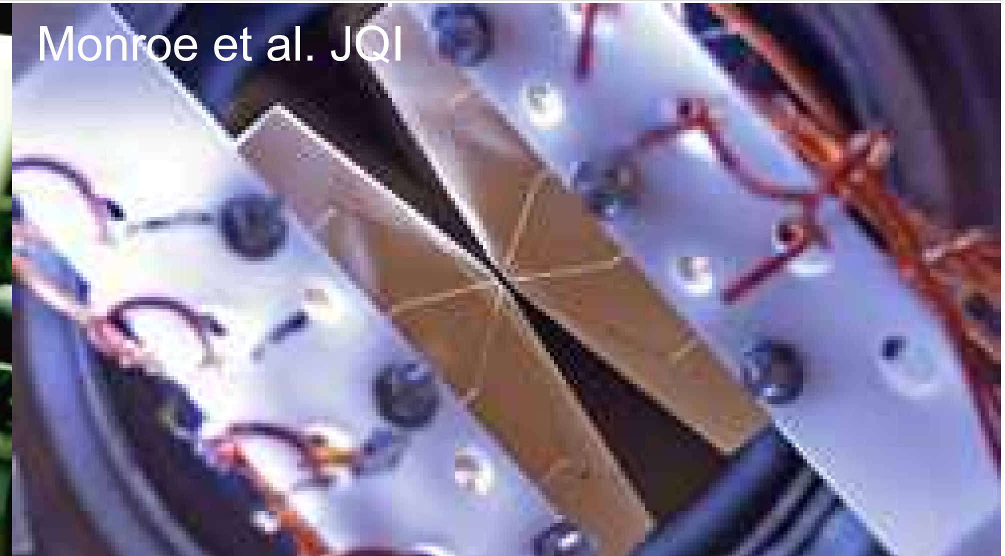

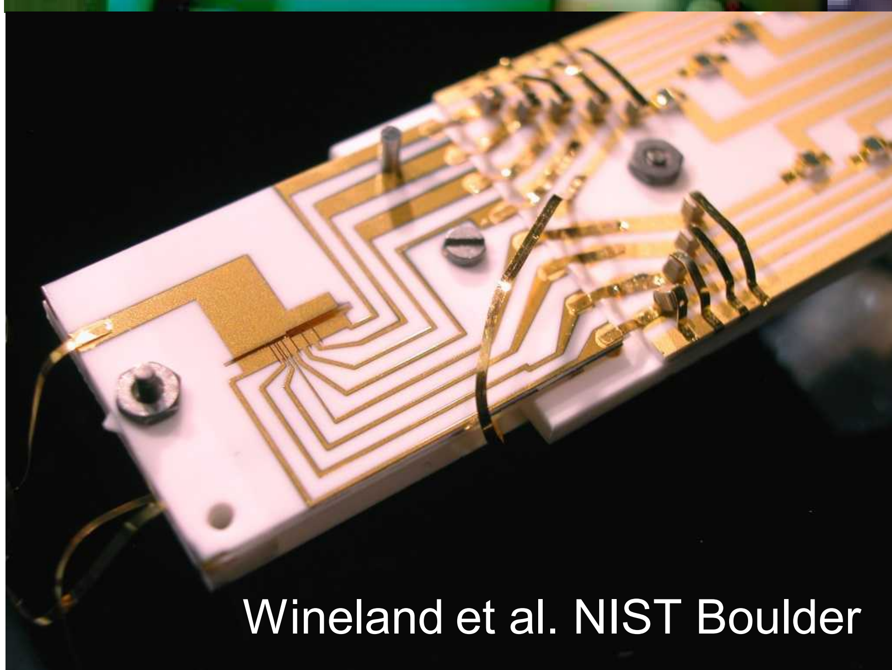

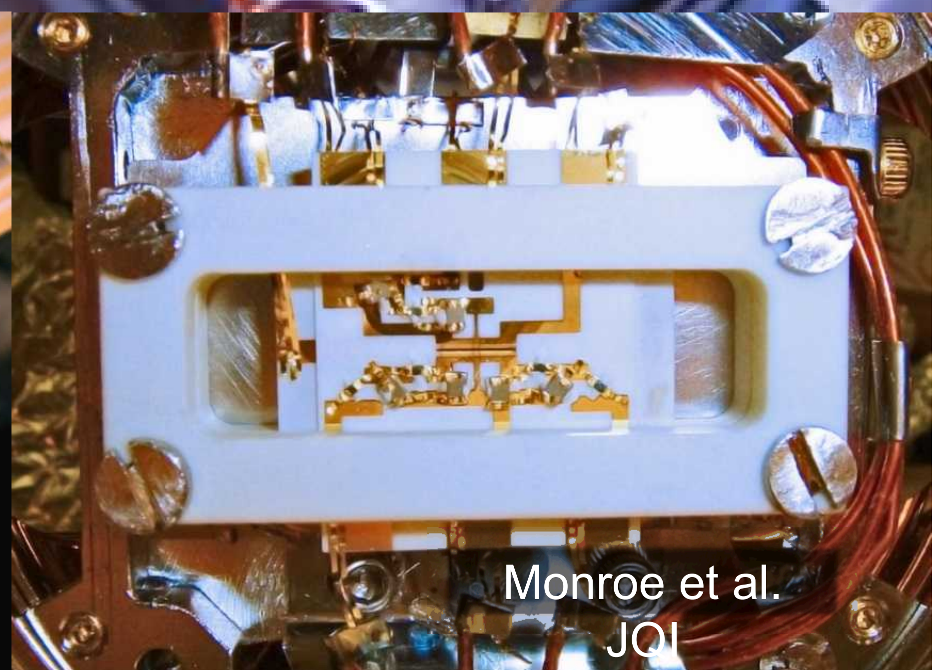

Heating rate Q-section

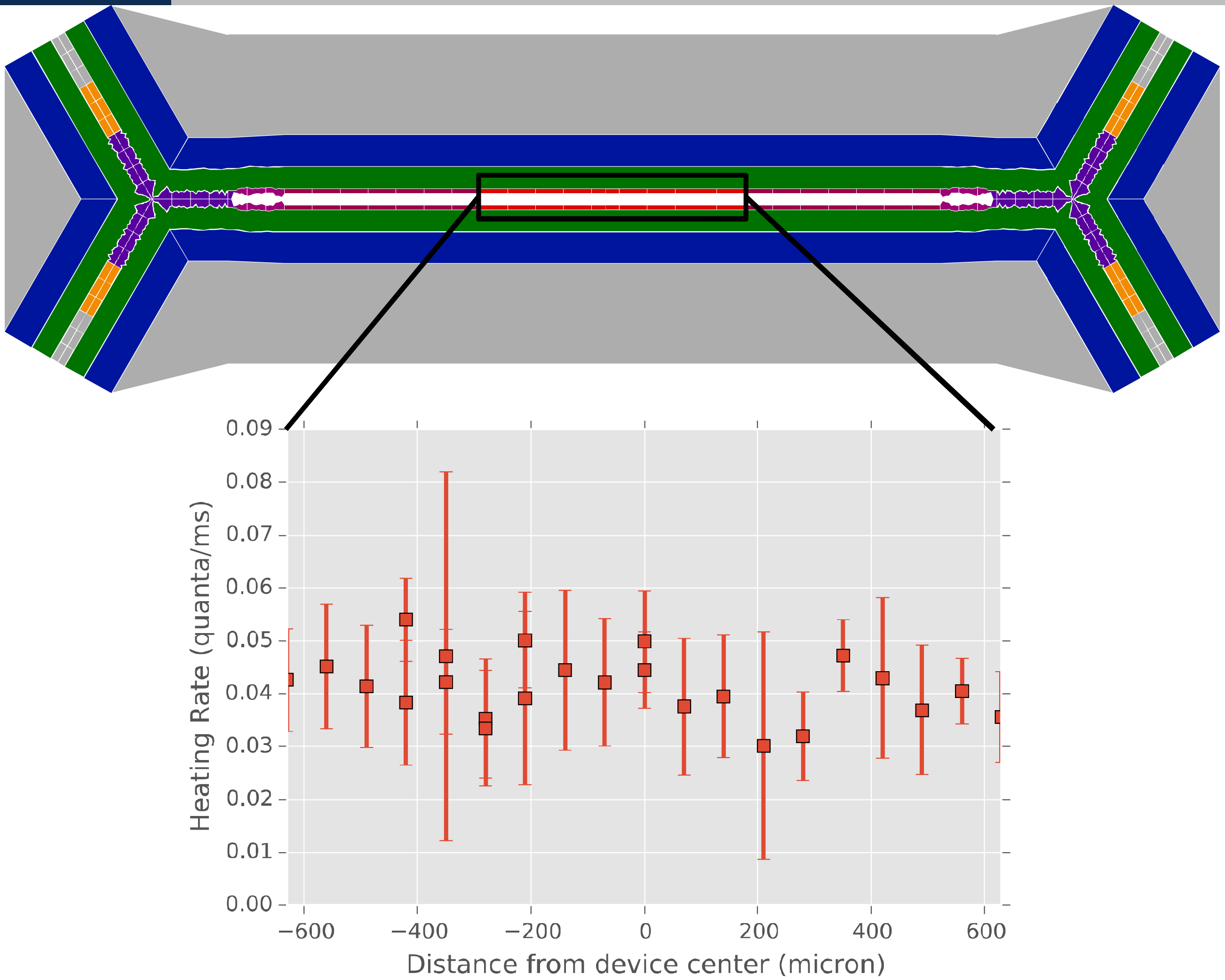

Heating rate 40q/s on average, $^{171}Yb^{+}$, Trap frequency 2.8 MHz, r.f. 50 MHz

Heating rate in HOA-2 is low and uniform along the length of the quantum section

GST debugging of the setup

GST characterizes the implemented processes and helps identify problems

$X_{\pi/2}$ and $Y_{\pi/2}$ gates implemented using BB1 pulse sequence

4/17: Markovianity violation

- Improve passive stability
- Add drift control of π-times

12/2: Improved X and Y gates, identity is worst

- Decoupled identity using X_π $W_{1.25\pi}$ $-X_\pi$ $W_{1.25\pi}$
- Switched to HOA-2 trap

2/9: Gates improved, systematic over-rotation detected

- Improve calibration of BB1 pulses
- Drift control of qubit frequency

3/2: X and Y gates are good, identity is still worst

- Implement identity as X_π Y_π X_π Y_π

3/30: Process fidelity of all gates <6×10^{-5}

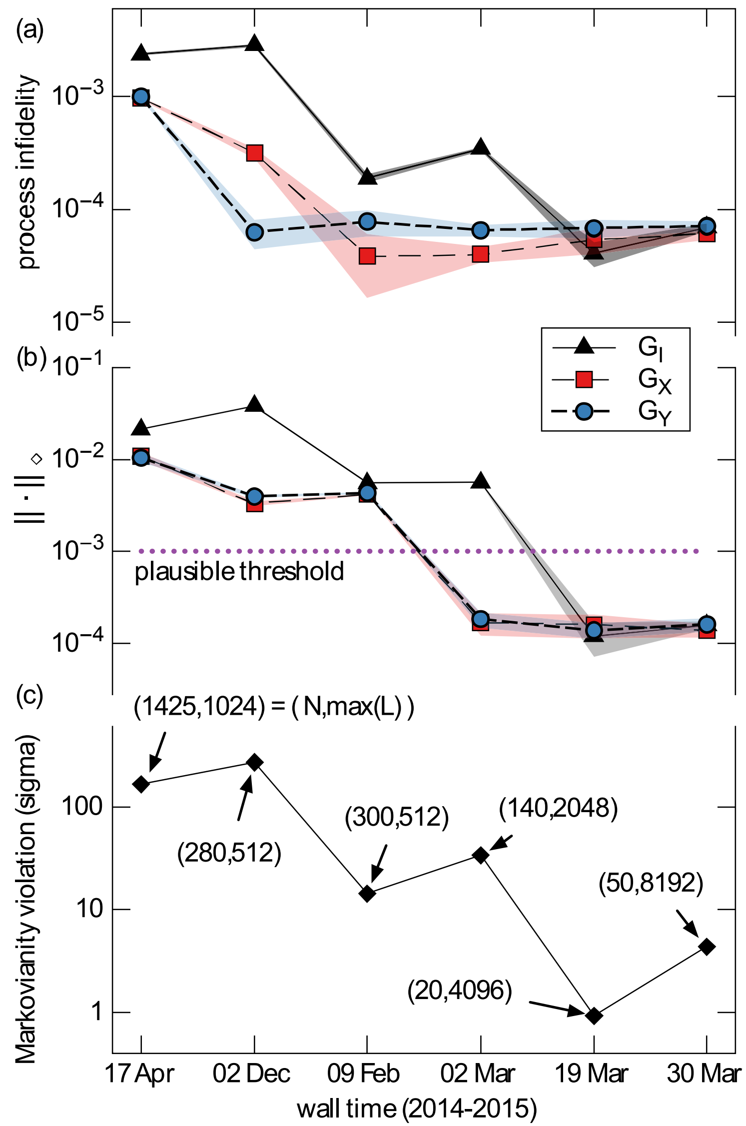

HOA-2 calcium

- Axial trap frequency as function of gain on dc control voltages
- Approximated by square root with single fit parameter

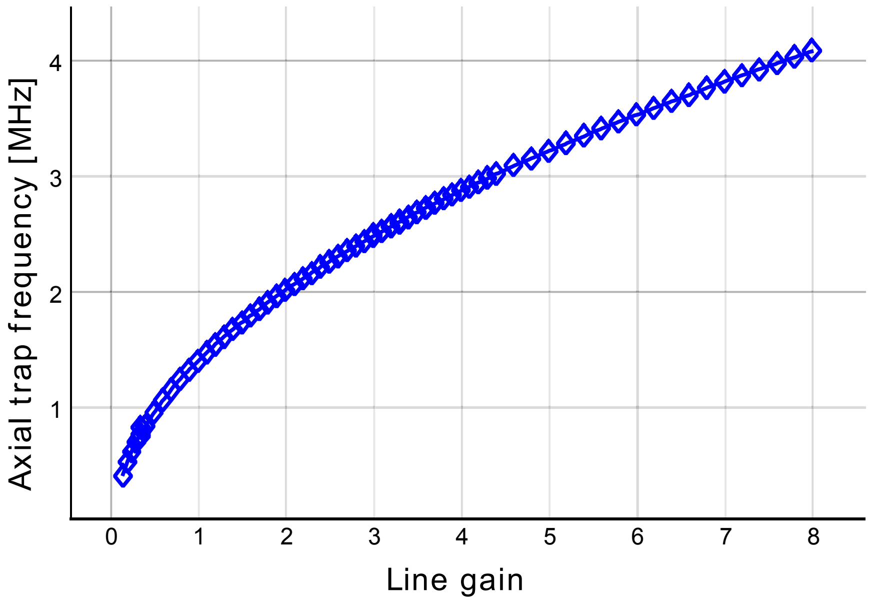

- Radial trap frequencies up to 8MHz demonstrated with rf frequency of 49MHz

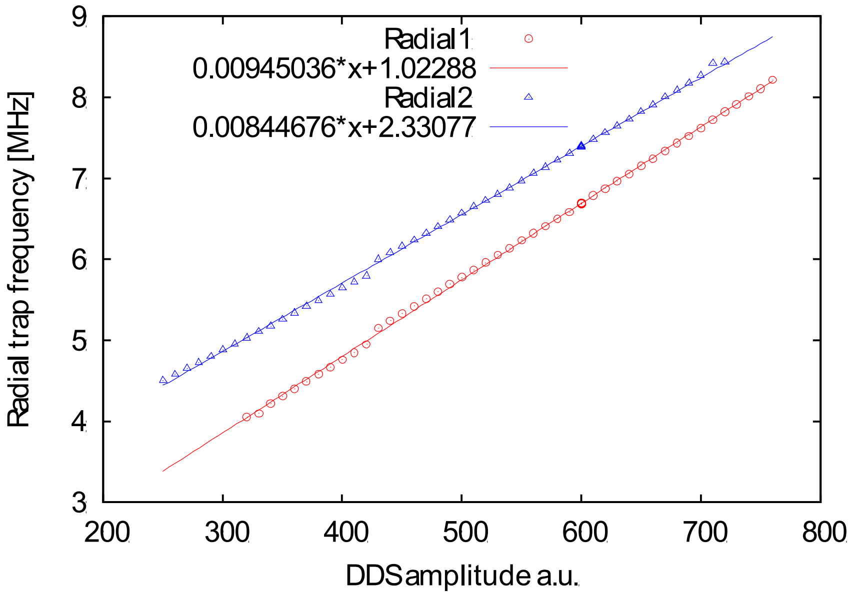

Compensation Q-section

Compensation field varies slowly along linear quantum section of the trap

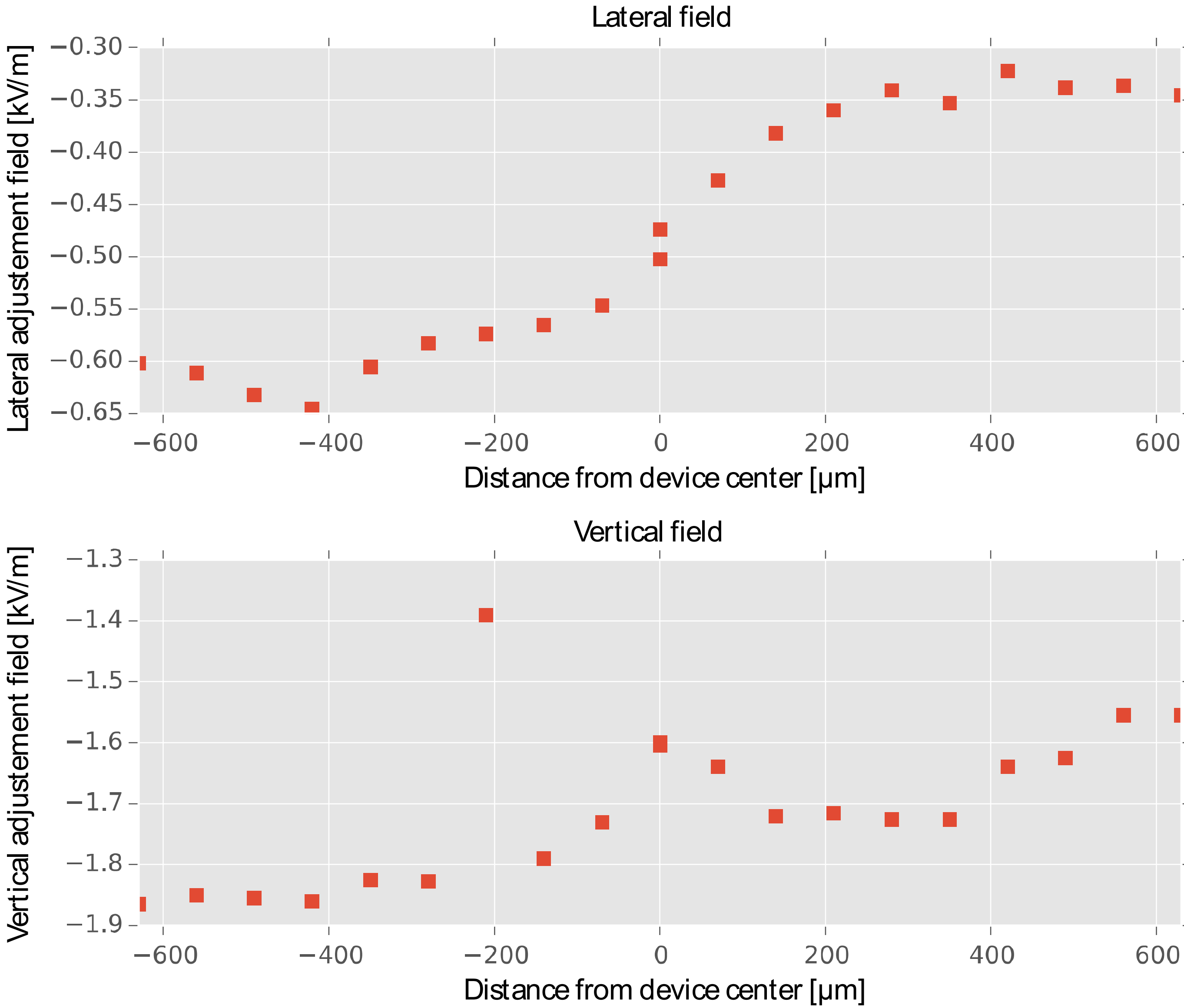

GST: debugging

February 9

Gate	Eigenvalues	Fixed pt	Rotn. axis	Angle	Diag. decay	Off-diag. decay
Gi	1 0.9999 $0.9996e^{i0.0}$ $0.9996e^{-i0.0}$	0.9775 0.0004 −0.2107 0.0063	0.5252 −0.009 0.8506 −0.0244	0.001699π	0.000121	0.000365
Gx	$1e^{i1.6}$ $1e^{-i1.6}$ 1 0.9999	1 0 −0.0003 0.0017	-3×10^{-6} −1 -3×10^{-5} −0.0009	0.501308π	0	0.000046
Gy	$0.9999e^{i1.6}$ $0.9999e^{-i1.6}$ 0.9999 0.9999	−0.9896 0.0008 0.1437 −0.0016	−0.2474 0.0001 0.9689 −0.0001	0.501366π	0.000109	0.000136

March 2

Gate	Eigenvalues	Fixed pt	Rotn. axis	Angle	Diag. decay	Off-diag. decay
Gi	$0.9993e^{i0.0}$ $0.9993e^{-i0.0}$ 1 0.9999	1 0 0.289 0.0053	−0.0035 0.014 −0.9999 0.0006	0.001769π	0	0.000739
Gx	$0.9999e^{i1.6}$ $0.9999e^{-i1.6}$ 1 1	1 0 −0.0002 0.0016	-3×10^{-5} −1 0.0001 0.0006	0.500007π	0	0.000068
Gy	$0.9999e^{i1.6}$ $0.9999e^{-i1.6}$ 1 0.9999	1 0 5.0976 0.0034	0.1104 -4×10^{-5} 0.9939 0.0005	0.50001π	0	0.000084

Sandia National Laboratories

GST: microwave single qubit gates

Comparison of the different implementations of the identity gate:

Experimental run	Process infidelity $\times 10^3$			1/2 Trace distance $\times 10^3$		
	G_I	G_X	G_Y	G_I	G_X	G_Y
wait	0.02 ± 0.5	0.31 ± 0.12	0.49 ± 0.009	0.49 ± 0.53	3.0 ± 0.12	3.9 ± 0.1
BB1 wait	1.4 ± 1.2	0.19 ± 0.18	0.06 ± 0.49	4.6 ± 0.9	3.5 ± 4	2.5 ± 0.3
BB1 XX	1.2 ± 1.4	0.1 ± 0.16	0.035 ± 0.017	7.4 ± 1.8	3.6 ± 2.2	2.4 ± 0.8
BB1 XYXY	0.06 ± 0.16	0.06 ± 0.08	0.06 ± 0.04	0.07 ± 0.17	1.3 ± 1.5	1.2 ± 0.9

GST: Raman laser qubit control

Raw data poor gates

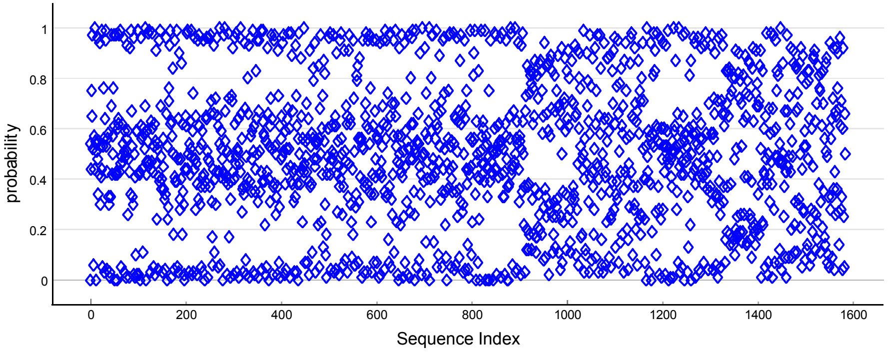

Raw data good gates

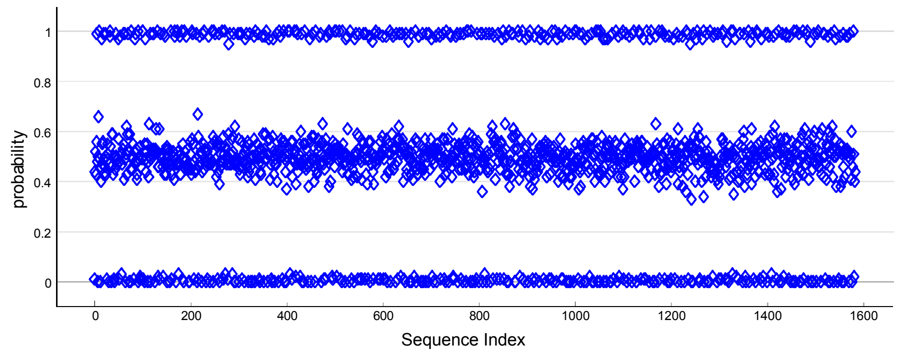

Experimental Parameters				Infidelity $\times 10^4$		Trace Distance $\times 10^3$	
Beam Orientation	Drift Control	Compensated Gates	Gapless	Gi	max(Gx,Gy)	Gi	max(Gx,Gy)
$\Rightarrow$				0.16	11	1.3	7.1
$\Rightarrow$	✓			0.14	7.3	1.3	6.6
$\Rightarrow$		Gi, Gx, Gy		16.2	1.7	27	3.0
$\Rightarrow$	✓	Gi, Gx, Gy		10.5	2.0	15	4.0
$\Rightarrow$	✓	Gx, Gy		0.05	1.7	1.2	4.0
$\Rightarrow$	✓	Gi, Gx, Gy	✓	1.28	0.5	0.49	2.6
$\rightleftharpoons$		Gi, Gx, Gy	✓	11.1	4.1	2.3	2.7
$\rightleftharpoons$		Gx, Gy	✓*	0.89	5.8	8.8	2.3

High intensity laser close to trap surface does NOT lead to problems

GST on symmetric subspace

Basic gates: G_I

$$G_{XX} = G_X \otimes G_X$$

$$G_{YY} = G_Y \otimes G_Y$$

$$G_{MS}$$

Preparation Fiducials:

- $\{\}$
- G_{XX}
- G_{YY}
- G_{MS}
- $G_{XX}G_{MS}$
- $G_{YY}G_{MS}$

Germs:

- G_I
- G_{XX}
- G_{YY}
- G_{MS}
- $G_I G_{XX}$
- $G_I G_{YY}$
- $G_I G_{MS}$
- $G_{XX}G_{YY}$
- $G_{XX}G_{MS}$
- $G_{YY}G_{MS}$
- $G_I G_I G_{XX}$
- $G_I G_I G_{YY}$

Detection Fiducials:

- $\{\}$
- G_{XX}
- G_{YY}
- G_{MS}
- $G_{XX}G_{MS}$
- $G_{YY}G_{MS}$
- G_{XX}^3
- G_{YY}^3
- $G_{YY}^2 G_{MS}$

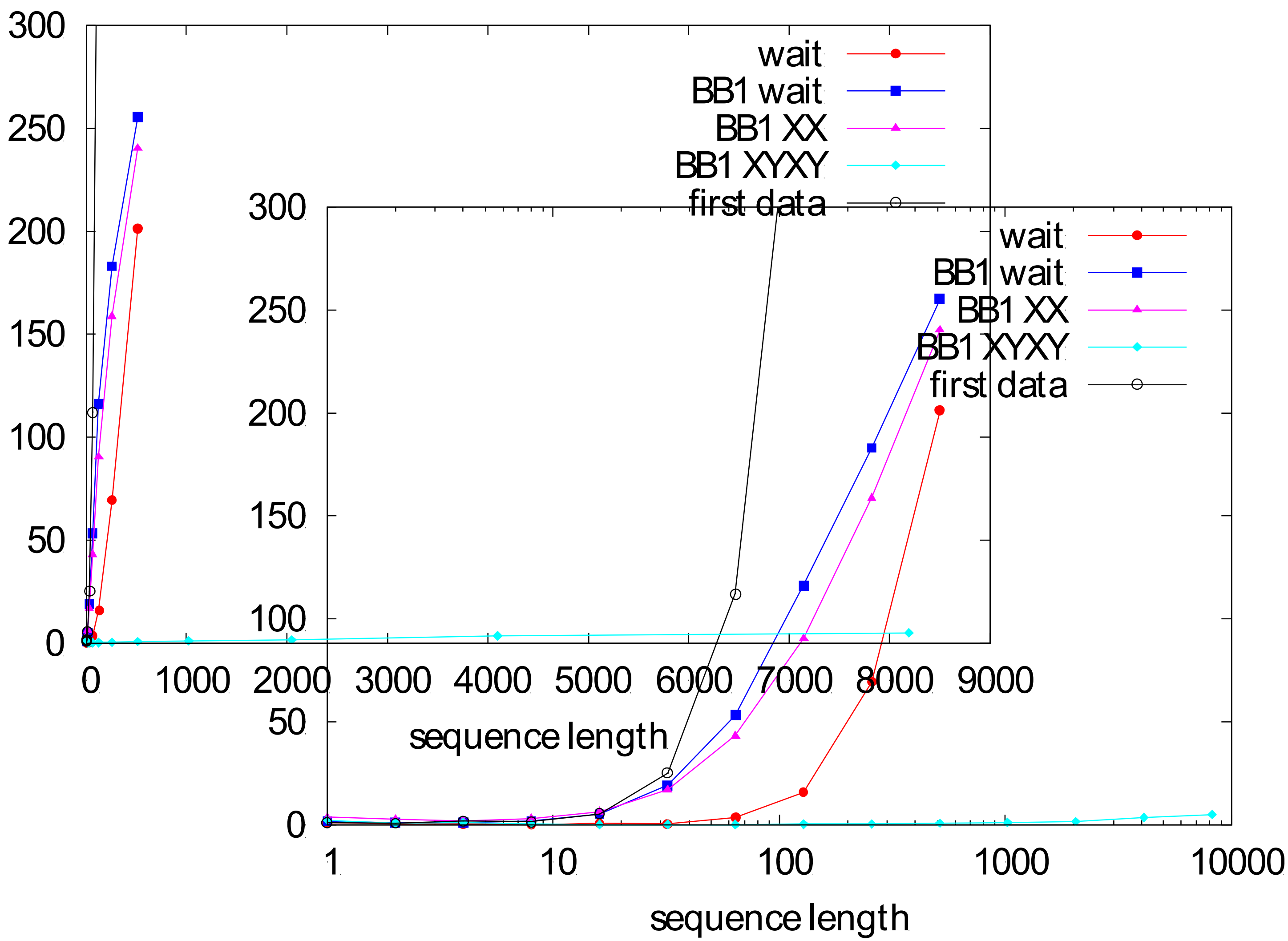
300
250
200
150
100
50
0
0
1000
2000
3000
4000
5000
6000
7000
8000
9000
sequence length
wait
BB1 wait
BB1 XX
BB1 XYXY
first data
300
250
200
150
100
50
0
1
10
100
1000
10000
sequence length
wait
BB1 wait
BB1 XX
BB1 XYXY
first data

HOA-2 heating rates

Heating rates as function of principal axes rotation

- Principal axes rotation measured by measuring π-times of Rabi flopping on cooled motional modes
- Minimal heating rates for motional $\dot{n}_\parallel$ mode parallel to trap surface
- Without technical noise: $\dot{n}_\perp \leq 2\dot{n}_\parallel$ Vertical mode has as most
- Limited by technical noise

$^{171}Yb^+$, Trap frequency 2.8 MHz, r.f. 50 MHz

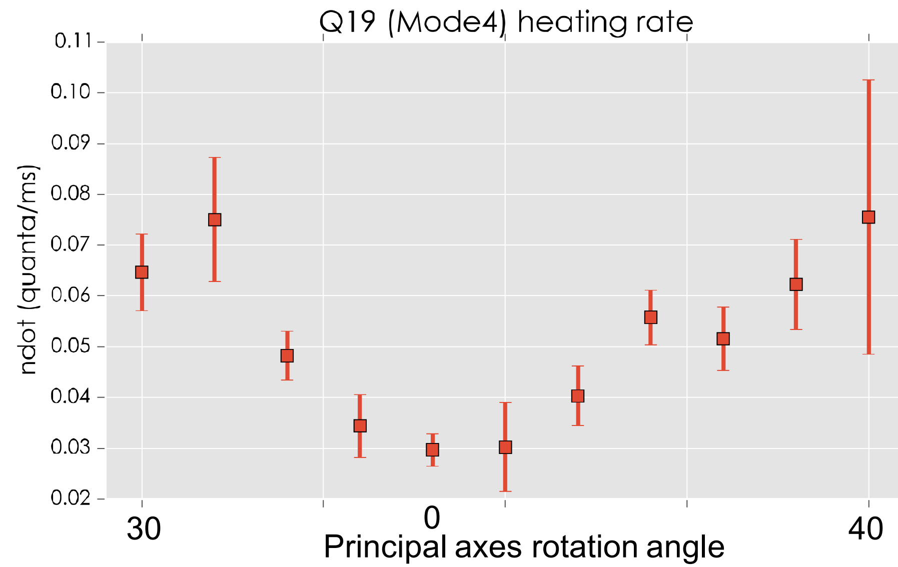

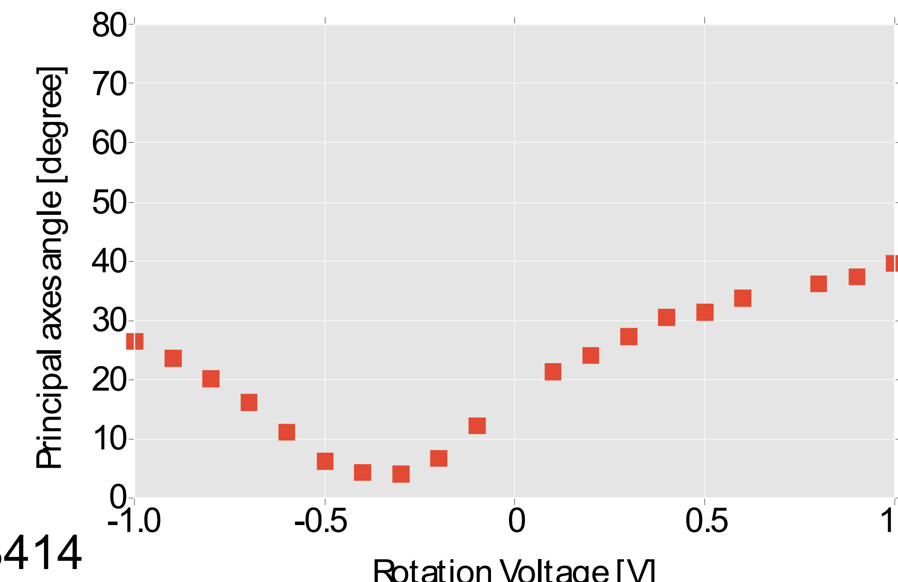

P. Schindler, et al., Phys. Rev. A **92**, 013414

Pulsed laser Raman transitions

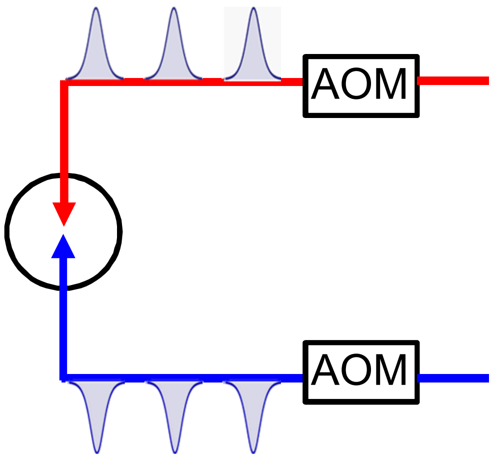

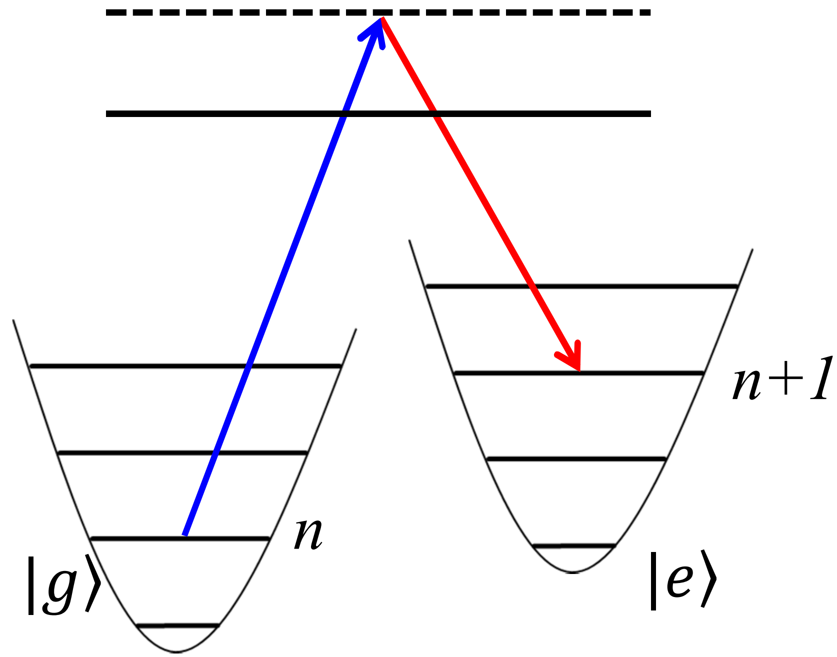

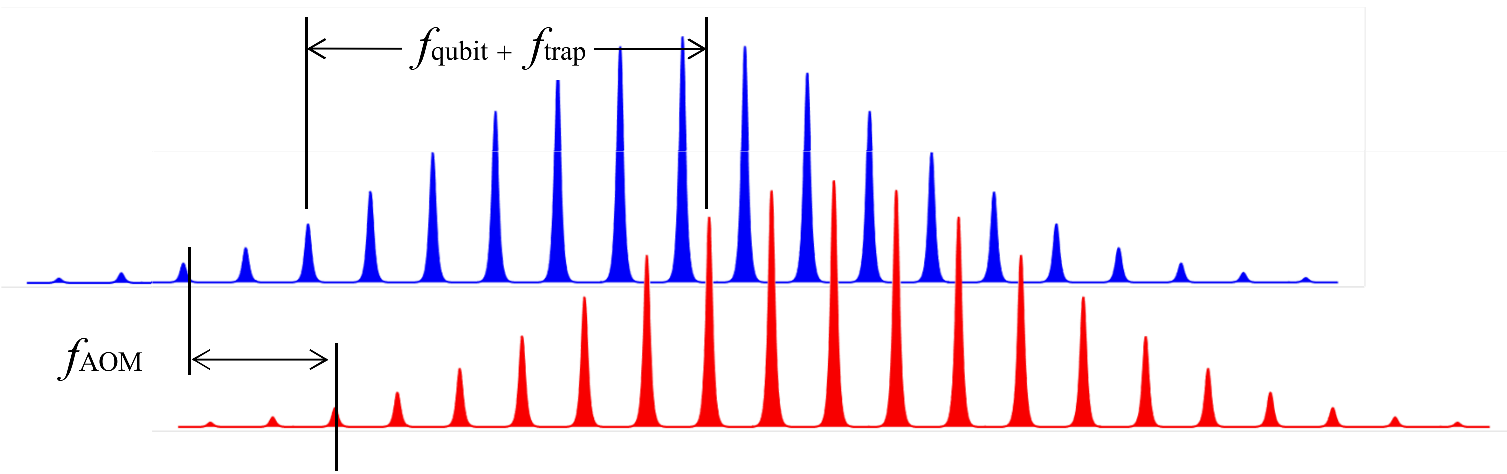

Pulsed laser Raman transitions

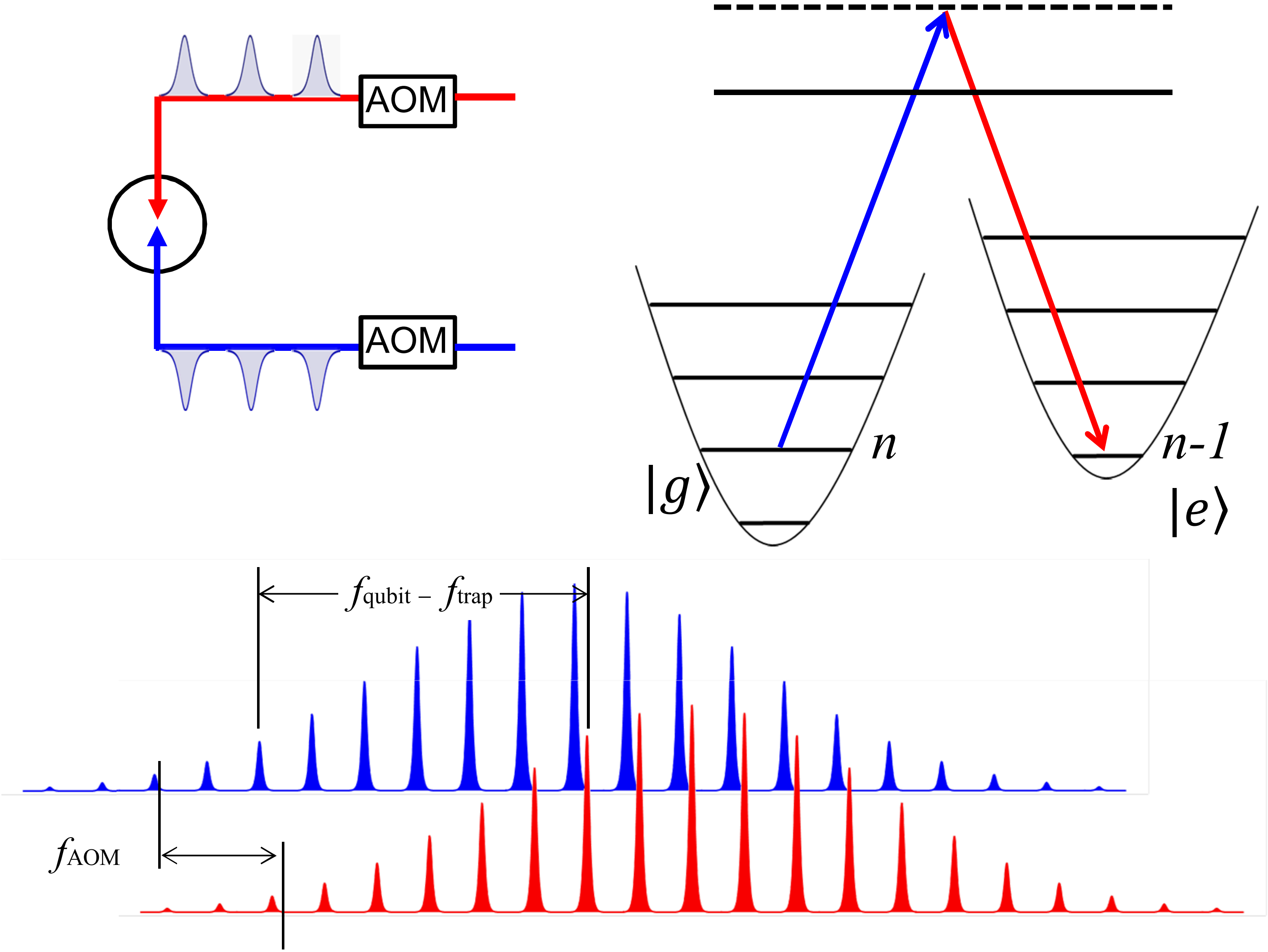

Sideband cooling

- Ground state cooling evident when red sideband cannot be driven
- Data shows ground state cooling of two ion radial tilt mode, $\bar{n} \ll 1$

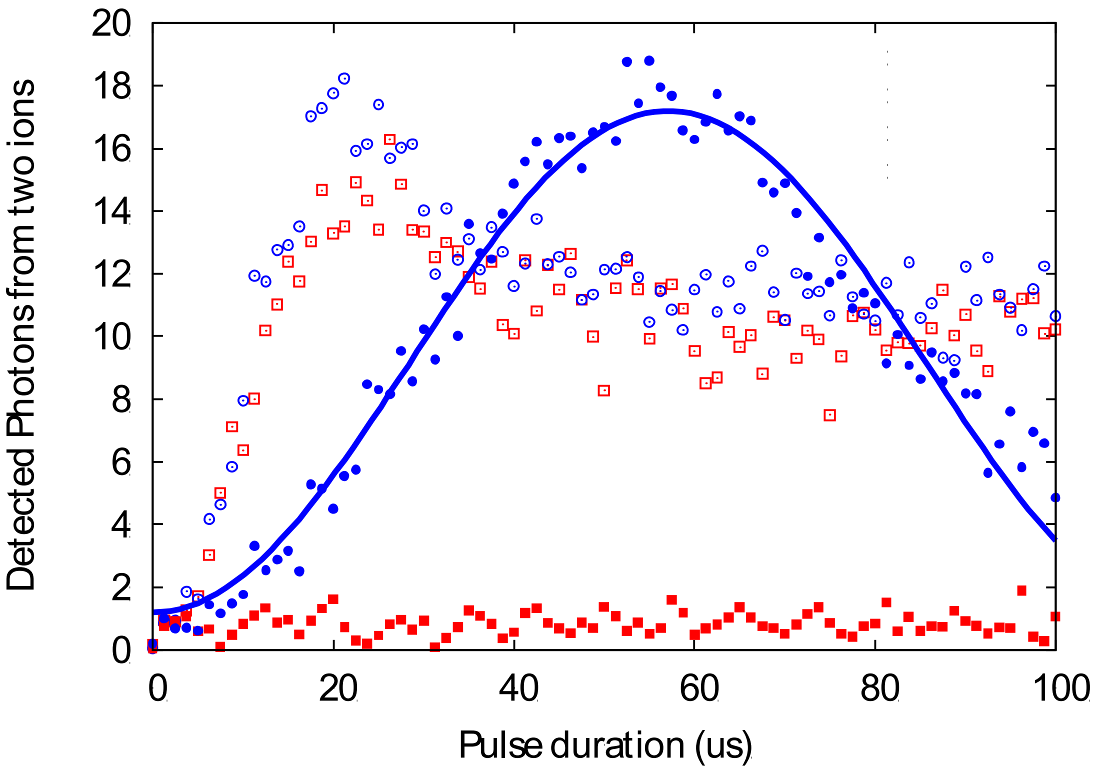

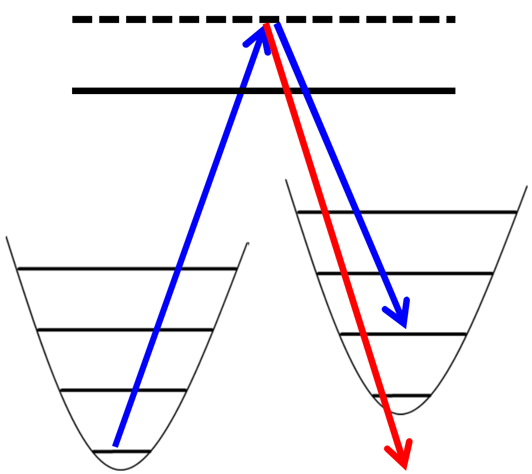

Entangling Gate

Basic idea: Use common motion of the ions to mediate entanglement

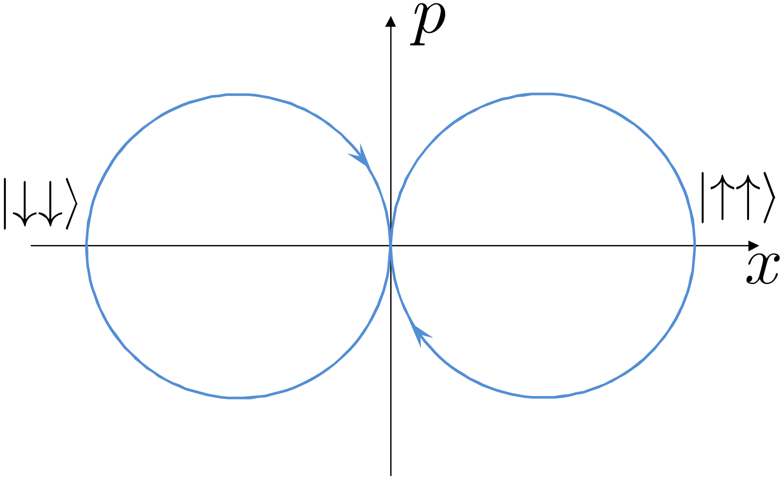

- Raman beams create *spin-dependent force*
- Force drives the ions away from and then back to their starting position

- Spin dependent phase remains

[1] K. Mølmer, A. Sørensen, PRL 82, 1835 (1999)
[2] A. Sørensen, K. Mølmer, PRL 82, 1971 (1999)
[3] A. Sørensen, K. Mølmer, PRA 62, 022311 (2000)

Two-qubit gate tomography